DESIGNING FOR SUSTAINABILITY WITH CO_2-TUNABLE SOLVENTS

A Dissertation
Presented to
The Academic Faculty

by

Jackson Walker Ford

In Partial Fulfillment
of the Requirements for the Degree
Doctor of Philosophy in the
School of Chemical and Biomolecular Engineering

Georgia Institute of Technology
December 2007

DESIGNING FOR SUSTAINABILITY WITH CO_2-TUNABLE SOLVENTS

Approved by:

Dr. Charles A. Eckert
School of Chemical and Biomolecular Engineering
Georgia Institute of Technology

Dr. Charles L. Liotta
School of Chemistry and Biochemistry
Georgia Institute of Technology

Dr. Victor Breedveld
School of Chemical and Biomolecular Engineering
Georgia Institute of Technology

Dr. Dennis W. Hess
School of Chemical and Biomolecular Engineering
Georgia Institute of Technology

Dr. Amyn Teja
School of Chemical and Biomolecular Engineering
Georgia Institute of Technology

Date Approved: October 30, 2007

For Christine

ACKNOWLEDGEMENTS

I am indebted to a number of people who assisted and inspired this work. Dr. Chuck Eckert and Dr. Charlie Liotta have been a constant source of ideas, advice, and constructive criticism during my time at Georgia Tech. Your give-and-take collaboration is a privilege to observe, not to mention great entertainment at times. Both of you have been great examples for me to follow as I begin my academic career.

The entire Eckert-Liotta research group shares the credit for this work. Thanks for your willingness to help, your great ideas, and your friendship. In particular, I'd like to thank Dr. Jie Lu (Julie) for her countless hours reviewing my data, explaining new techniques, looking over Powerpoint slides, and reading my papers and chapters. You will make an incredible professor, Julie, and I am honored to have worked with you. I'd also like to thank Dr. Jason Hallett, who contributed significantly to the OATS project. Dr. Pamela Pollet was a fount of knowledge on the NMR/ligand work, and Dr. Daniele Vinci and Dr. Veronica Llopis-Mestre were also helpful with some chemistry-related issues. A special thanks also to Deborah Babykin, who is a tremendous help in a number of areas. Thanks to all of you for your patience, diligence, and can-do attitude to help complete these projects.

Several undergraduate researchers made significant contributions with these experiments: David Meyer, Laura Nuñez, and Kierston Shill. You did a lot of the "grunt work" and I thank you for working hard and being patient at times as I tried to figure out what to do next.

I am grateful to Dr. Sergei Kazarian for his help and advice on IR measurements for examining the complexes in Chapter II. I also appreciate Dr. Leslie Gelbaum's assistance with the NMR measurements and data analysis in Appendix A.

I thank my family, which has inspired me to make the best of every opportunity. This experience at Georgia Tech has been challenging, and I have depended on your encouragement, advice, and support.

Finally, and most importantly, I thank my wife Christine. You have made immeasurable sacrifices to help me reach this point. Your constant love and encouragement have given me the strength and motivation I needed to finish this work. Thanks for putting up with the uncertainty and stress of the last few years. Regardless of what happens from here on, my proudest achievement will be convincing you to marry me. I love you.

TABLE OF CONTENTS

LIST OF TABLES

LIST OF FIGURES

LIST OF SYMBOLS

α	Kamlet-Taft hydrogen-bonding acidity
A_0	initial amount of substrate
β	Kamlet-Taft hydrogen-bonding basicity
B_∞	final amount of product
c	speed of light
C_1, C_2	fitting constants
^{13}C	carbon-13
E_T	transition energy
h	Planck's constant
k_{obs}	pseudo-first-order rate constant
k_2	second-order rate constant
λ	wavelength
N_A	Avogadro's number
ν	wavenumber
π^*	Kamlet-Taft dipolarity/polarizability
^{31}P	phosphorus-31
r^2	correlation coefficient
t	time
vol.%	volume percent
x_i	mole fraction of species i
$x_{i,local}$	local mole fraction of species i
$x_{i,bulk}$	bulk mole fraction of species i
Z	Kosower's polarity parameter

LIST OF ABBREVIATIONS

B	branched isomer
CEF	composition enhancement factor
FID	flame ionization detector
GAS	gas-antisolvent
GC	gas chromatography
GXL	gas-expanded liquid
HPLC	high-performance liquid chromatography
IR	infrared
L	linear isomer
LSER	Linear Solvation Energy Relationship
MNBS	methyl *p*-nitrobenzenesulfonate
MS	mass spectrometry
NMR	nuclear magnetic resonance
OATS	Organic-Aqueous Tunable Solvents
PID	proportional-integral-derivative
PTAD	4-phenyl-1,2,4-triazoline-3,5-dione
PTFE	polytetrafluoroethylene
SFC	supercritical fluid chromatography
S_N2	nucleophilic bimolecular substitution
STP	standard temperature and pressure
TBA	tributylamine
THF	tetrahydrofuran
TOF	turnover frequency
TPP	triphenylphosphine

TPPDS	triphenylphosphine disulfonate
TPPMS	triphenylphosphine monosulfonate
TPPTS	triphenylphosphine trisulfonate
UHP	ultra high purity
UV-Vis	ultraviolet-visible

SUMMARY

Developing greener, more efficient, and less energy-intensive processes will lead the chemical industry into a more sustainable future. Gas-expanded liquids (GXLs) form a unique class of environmentally benign and tunable solvents that can be used in a variety of applications. Through the series of studies presented in this thesis, we have investigated both the properties and applications of GXLs. We have developed a more complete understanding of the interactions between the gas, the organic liquid, and solutes at the molecular level through kinetic and solvatochromic experiments. We have examined a Diels-Alder reaction and an S_N2 reaction and have described the kinetic results in terms of intermolecular interactions and local composition enhancement. We have also demonstrated the use of Organic-Aqueous Tunable Solvents, a special case of GXLs, to recycle homogeneous hydroformylation catalysts. The results of this research can be used to guide future applications of GXLs as green reaction solvents.

CHAPTER I

INTRODUCTION

Sustainable development requires that efforts to conserve, recycle, and reuse scarce resources accompany the growth of populations and economies. To meet these challenges, new technologies are needed to create better products more efficiently, using renewable or abundant resources whenever possible. This point applies particularly to the chemical processing industry, which depends to a great extent on nonrenewable, petroleum-derived resources.

Within the chemical processing industry, a major portion of both equipment and operating cost relates to separating reactants, products, catalysts, and solvents. The massive amounts of energy required and the use of toxic or dangerous solvents in these separations often pose undesirable environmental impacts. As a result, designing for efficient and environmentally-friendly separations is one of the core principles of green engineering.[1, 2] While distillation has long been, and will likely continue to be, the workhorse unit operation in commodity chemical production, other separation techniques become more viable at the smaller scales and higher purity requirements of fine chemicals and pharmaceuticals production.

An area of intense research related to separations is the use of more benign alternative solvents rather than traditional organic liquids. These alternative solvents include supercritical fluids, near-critical water, and ionic liquids. This thesis examines two additional alternative solvent systems: gas-expanded liquids and organic-aqueous tunable solvents. These solvent systems have the potential to reduce the environmental

footprint and improve the sustainability of chemical production through reducing waste, utilizing abundant and cheap CO_2, and enabling less energy-intensive separations to recover products and catalysts.

Gas-expanded liquids (GXLs), organic liquids expanded by CO_2, are a novel class of green solvents offering many advantages over traditional organic solvents, including favorable solvent strength and transport properties that are highly tunable with simple pressure variations. GXLs have the potential to greatly reduce the amounts of organic solvents used in chemical processing. As evidenced by a recent review by Jessop and Subramaniam, much research has been done to examine the properties and applications of GXLs.[3] However, a critical gap in the literature exists relative to molecular-level understanding of the interactions between the organic liquid, the gas, and dilute solutes. In Chapters II-III of this work, we seek to expand the fundamental understanding of these interactions as they relate to two model reactions in GXLs. Better understanding of the microscopic behavior of these solvents could lead to more effective and widespread industrial implementation of GXLs.

The first of these studies (Chapter II) examines a Diels-Alder reaction in CO_2-expanded acetonitrile: the reaction of anthracene and 4-phenyl-1,2,4-triazoline-3,5-dione (PTAD). This reaction has been used to probe solvent effects in organic liquids and supercritical fluids previously.[4, 5] We monitor this reaction using *in situ* high-pressure fluorescence spectroscopy. We compare these kinetic results to solvatochromic measurements using Linear Solvation Energy Relationships (LSERs) to describe quantitatively the impacts of solvent-solvent and solvent-solute interactions on this reaction in CO_2-expanded acetonitrile.

In Chapter III we analyze the S_N2 reaction of tributylamine with methyl *p*-nitrobenzenesulfonate, also in CO_2-expanded acetonitrile. This Menschutkin reaction is considered an excellent probe of local solvent polarity, due to its charge-separated transition state. We use *in situ* high-pressure UV-Vis spectroscopy to follow this reaction, and compare the results to other measures of bulk and local polarity to develop a clearer picture of the role of intermolecular interactions in this reaction.

Chapters IV-V relate to a special case of GXLs, Organic-Aqueous Tunable Solvents (OATS). The OATS system consists of a miscible organic-aqueous phase during reaction followed by a CO_2-induced downstream phase separation, which facilitate product isolation and catalyst recycle. The key feature of this system is that CO_2 associates more strongly with the organic components than the aqueous components, forcing a phase separation to form a gas-expanded organic-rich phase and a water-rich phase. The process strategy of OATS enables homogeneous reactions involving water-soluble catalysts and hydrophobic reactants, allowing high reaction rates and selectivity but avoiding the often costly and environmentally unfriendly separation inherent for homogeneous catalysis.

Previous work in the Eckert-Liotta group has demonstrated the effectiveness of the OATS system to recycle both organometallic catalysts and enzyme biocatalysts.[6-8] In Chapter IV, we use the OATS system to recycle organometallic catalysts in the hydroformylation of 1-octene. The OATS system overcomes several of the limitations associated with hydroformylation of long-chain alkenes, including improved solubility of reactants and products and facile catalyst recovery.[9-11]

In Chapter V, we implement OATS in the catalytic hydroformylation of *p*-methylstyrene. This reaction demonstrates the versatility of the OATS system for hydroformylations, i.e. it demonstrates flexibility for both aliphatic and aromatic compounds, and tunability for both linear and branched products. We examine factors influencing both the reaction and the separation. We also present a path forward for future work on this ongoing project.

We present the conclusions developed in this work and give some direction for future work on these or related projects in Chapter VI.

Finally in Appendix A, we seek to improve our understanding of the data presented in Chapter IV. A side reaction in the hydroformylation of 1-octene, the isomerization to other alkenes, lowered the yield of the desired products. Empirical evidence pointed to the choice of ligand as a source of this isomerization. In this appendix, we use ^{31}P NMR spectroscopy and electron density calculations in an attempt to clarify the role of increased ligand sulfonation on this side reaction.

References

1. Anastas, P. T.; Warner, J. C., *Green Chemistry: Theory and Practice*. Oxford University Press Inc.: New York, NY, 1998.

2. Anastas, P. T.; Zimmerman, J. B., Design through the 12 principles of green engineering. *Env. Sci. & Tech.* **2003,** *37* (5), 94A.

3. Jessop, P. G.; Subramaniam, B., Gas-expanded liquids. *Chem. Rev.* **2007,** *107*, 2666.

4. Konovalov, A. I.; Breus, I. P.; Sharagin, I. A.; Kiselev, V. D., Study of solvation effects in Diels-Alder reactions of 4-phenyl-1,2,4-triazoline-3,5-dione with anthracene and trans,trans-1,4-diphenyl-1,3-butadiene. *Zhurnal organicheskoi khimii* **1979,** *15* (2), 361.

5. Thompson, R. L.; Glaser, R.; Bush, D.; Liotta, C. L.; Eckert, C. A., Rate variations of a hetero-Diels-Alder reaction in supercritical fluid CO_2. *Ind. Eng. Chem. Res.* **1999,** *38*, 4220.

6. Jones, R. S. Carbon dioxide as a benign solvent for homogeneous catalyst recovery and recycle. Ph.D. Thesis, Georgia Institute of Technology, Atlanta, GA, 2005.

7. Hill, E. M.; Broering, J. M.; Hallett, J. P.; Bommarius, A. S.; Liotta, C. L.; Eckert, C. A., Coupling chiral homogeneous biocatalytic reactions with benign heterogeneous separation. *Green Chem.* **2007,** *9*, 888.

8. Lu, J.; Lazzaroni, M. J.; Hallett, J. P.; Bommarius, A. S.; Liotta, C. L.; Eckert, C. A., Tunable solvents for homogeneous catalyst recycle. *Ind. Eng. Chem. Res.* **2004,** *43*, 1586.

9. Robbins, G. P.; Hallett, J. P.; Bush, D.; Eckert, C. A., Liquid–liquid equilibria and partitioning in organic–aqueous systems. *Fluid Phase Equilibria* **2007,** *253*, 48.

10. Kohlpaintner, C. W.; Fischer, R. W.; Cornils, B., Aqueous biphasic catalysis: Ruhrchemie/Rhone-Poulenc oxo process. *Appl. Catal. A: Gen.* **2001,** *221*, 219.

11. Cornils, B., Exciting results from the field of homogeneous two-phase catalysis. *Angew. Chem. Intl. Ed. Engl.* **1995,** *94* (15), 1575.

CHAPTER II

SOLVENT EFFECTS ON THE KINETICS OF A DIELS-ALDER REACTION IN GAS-EXPANDED LIQUIDS

Introduction

Gas-expanded liquids (GXLs), organic liquids expanded under CO_2 pressure, are a novel class of sustainable solvents which offer many advantages over both traditional organic solvents and supercritical fluids. The solvent strength and transport properties of GXLs can be readily tuned with CO_2 pressure over a wide range intermediate between organic liquids and supercritical fluids.[1] Because GXLs contain up to 80 vol.% CO_2, they substantially reduce the need for organic solvent and are considered more environmentally desirable.[1-3] GXLs provide better mass transport than organic liquids, and have better solvent power compared to supercritical fluids.[1] GXLs operate at substantially lower pressures than supercritical fluids, typically 20-40 bars instead of 100-200, saving both capital costs and energy. Finally, GXLs facilitate less energy-intensive separations through depressurization to recover products and catalysts.

As a result of their tunability, GXLs can be applied in a number of industrially significant processes, including gas-antisolvent crystallization, nanoparticle formation, photoresist removal in microfabrication, and homogeneous catalyst recycling.[1, 3-7]

We have used CO_2-expanded acetonitrile as the solvent in this work. CO_2 is nontoxic, nonflammable, and an environmentally benign alternative to organic solvents. Acetonitrile is a polar aprotic solvent. We chose a polar solvent so that by adding the nonpolar solvent CO_2, the properties of the resulting GXL can be tuned over a wide

polarity range. In addition, an aprotic solvent was selected to avoid the formation of *in situ* acids, which could complicate the analysis.[8] Acetonitrile is also non-reactive with the solutes used in this research.

The cybotactic region is the volume immediately surrounding a solute molecule in which the local solvent structure is strongly affected by intermolecular forces between the solute and the solvent.[9, 10] The cybotactic region is often characterized by local composition and density enhancements.[11-15] Understanding how the local solvent structure changes with the solvent composition provides insight into optimizing reactions and separations in GXLs.

In this research the local structure of GXLs has been studied in kinetic and spectroscopic experiments. These processes are controlled by molecular interactions occurring in the local environment around either the spectroscopic probe molecule or the reactant/transition state of the reaction. Changes in the values of spectroscopically-measured solvatochromic probes, as well as reaction kinetics, can be attributed to the relative stabilization of one solute state over another by the solvent. In the case of solvatochromic probes, this stabilization is for the ground state of the molecule versus the excited state; for kinetic investigations, the relative stabilization of the reactants versus the reaction transition state becomes important.

Solvatochromic parameter values are obtained by measuring the solvent-dependent UV spectral shift of an indicator molecule (Refer to Figure 2.1 for structures of solvatochromic probe molecules used in this work).[10] The wavelength of maximum

(1)

(2)

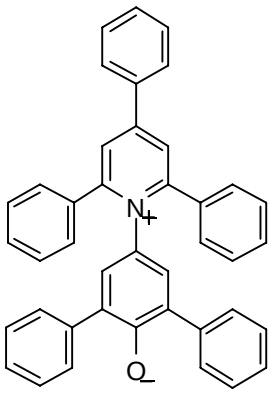

(3)

Figure 2.1: Solvatochromic probes: (1) *p*-nitroanisole (2) *p*-nitrophenol (3) Dimroth-Reichardt betaine dye.

absorption for the probe is dependent on the energy required to undergo a specific electronic transition.

A variety of solvatochromic scales exist which quantify various solvent properties.[10, 16-21] Solvatochromic parameters are useful for measuring certain interactions in the solute-organized cybotactic region, allowing segregation of various intermolecular forces. Although a number of scales are available for use, the well-developed solvatochromic parameters of Kamlet and Taft and Reichardt's $E_T(30)$ parameter were selected for this work.[16, 18, 21-24] The Kamlet-Taft solvatochromic parameters have been used previously to describe solvent effects in organic solvents,

near- and supercritical fluids, ionic liquids, and mixed solvents including gas-expanded liquids.[10, 17, 22-27]

The Diels-Alder reaction (See Figure 2.2) of anthracene and 4-phenyl-1,2,4-triazoline-3,5-dione (PTAD) has been studied in organic liquids and supercritical fluids as a model reaction to probe solvent properties.[28-30] The highly reactive dienophile PTAD facilitates short reaction times[31-34]. Anthracene concentration can be monitored *in situ* via either fluorescence or UV spectroscopy. Since neither PTAD nor the Diels-Alder adduct have a fluorescence signature, this spectroscopic technique is advantageous for simple but reliable analysis. Fluorescence spectroscopy enables detection of very dilute analyte concentrations ($<10^{-7}$ mol/L in this work), and allows pseudo-first order kinetic measurements without encountering the solubility limit of PTAD. Dilute solutions minimize the impact of the solutes on the bulk properties of the gas-expanded solvents under study.

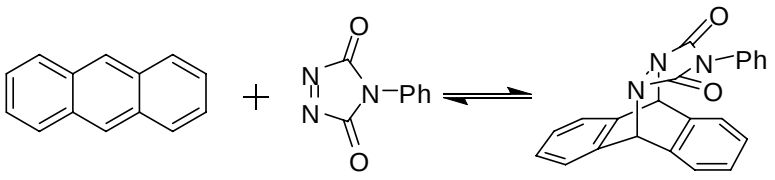

Figure 2.2: Diels-Alder reaction of anthracene with PTAD.

Linear Solvation Energy Relationships (LSERs) correlate the solvatochromic properties of solvents to a variety of configurational properties in solution such as solubility of a solute, rate of a reaction, thermodynamic properties, and chromatographic retention times, to name a few.[16, 17, 23] The LSER expression developed by Kamlet and Taft has been widely applied[16, 17, 35]:

$$XYZ = XYZ_0 + s\pi^* + a\alpha + b\beta \qquad \text{Equation 2-1}$$

where XYZ and XYZ_0 represent the magnitude of a solvent-dependent physicochemical property in a given solvent and in a reference solvent, respectively. The solvent-independent coefficients s, a, and b indicate the susceptibility of the property to the applied parameters. Multiple linear regression can be used to evaluate the coefficients XYZ_0, s, a, and b.

In this work, we use the Kamlet-Taft LSER to correlate kinetic data, specifically the natural logarithm of the second-order rate constant,

$$\ln k_2 = \ln k_{2,0} + s\pi^* + a\alpha + b\beta \qquad \text{Equation 2-2}$$

where k_2 is the rate constant of the Diels-Alder reaction of anthracene and PTAD in gas-expanded acetonitrile at a given CO_2 pressure, and $k_{2,0}$ is the rate constant in a reference solvent.

Experimental

Materials

Carbon dioxide (99.9995%) was purchased from Airgas and filtered prior to use. Acetonitrile (HPLC, ≥99.9%), p-nitroanisole (97%), p-nitrophenol (spectrophotometric grade), Reichardt's dye (~90%), 4-phenyl-1,2,4-triazoline-3,5-dione (98%), and anthracene (99%) were purchased from Sigma-Aldrich. All solvents and reagents were used as received.

Apparatus

Both kinetic and solvatochromic experiments were conducted in a stainless steel high pressure optical vessel, equipped with three sapphire windows arranged to allow *in situ* spectroscopic analysis. The vessel has a built-in circulating water jacket to control

temperature within ±0.1ºC of the setpoint using a constant temperature flow bath (Thermo Electron Corporation, Neslab RTE7). Vessel temperature was monitored via a thermocouple and readout (Omega). Vessel pressure was monitored using a pressure transducer and readout (Druck) with an uncertainty of ±1 psi. CO_2 was metered into the vessel using a syringe pump (ISCO, 260D). Agitation rate was controlled by a magnetic stir bar and motor (H+P Labortechnik, Variomag Telemodul 20C) throughout the measurements. Temperature and pressure gauges were calibrated to ensure their accuracy in these experiments.

For solvatochromic experiments, we measured the UV/vis spectra *in situ* using a Hewlett-Packard 8453 UV/vis spectrophotometer (Agilent Technologies).

In the kinetic experiments, we monitored anthracene fluorescence *in situ* during the course of the reaction via a fiber-optic fluorescence detector (Ocean Optics, USB 2000) with Ocean Optics OOIBase software. A mercury vapor short-arc lamp (Kratos Analytical, LH151) with a power supply (Kratos, LPS 255 HR) and monochromator (Kratos) enabled anthracene excitation at $\lambda = 350$ nm. Fluorescence spectra were detected over the range from 300 to 900 nm, with automated collection of fluorescence intensity data at specified wavelengths (accurate to within 0.4 nm) throughout the course of the reaction.

Procedure

For the solvatochromic experiments, we prepared concentrated stock solutions of each of the solvatochromic probe molecules in acetonitrile. We diluted a known volume of the stock solution into acetonitrile to achieve a UV response within the range of the detector. We sealed the cell and added CO_2 to the desired pressure. For each pressure

(i.e. each x_{CO2} value), we waited until the cell contents reached equilibrium before recording the UV spectrum. The solvatochromic parameter measurements reported here are based on multiple cell loadings and show consistent trends. Although we did not perform a comprehensive error analysis for the solvatochromic data in this study, the scatter of the data in Figures 2.3 through 2.6 gives an indication of the error rate.

We used the following procedure in our kinetic experiments. We loaded the cell initially with 5 mL of a 10^{-3} mol/L solution of PTAD in acetonitrile and then sealed and heated the cell to 40ºC. We added 50 μL of a 10^{-3} mol/L solution of anthracene in acetonitrile via a micro-pipetter and initiated the data logging on the computer. We then re-sealed the cell and loaded CO_2 to the desired pressure. For high CO_2 loadings (x_{CO2} > 0.80) we decreased the acetonitrile volumes of the initial loadings, but the initial concentration of the substrates in the resulting GXL prior to reaction was the same in all cases. We corrected the concentrations of PTAD and anthracene for solvent volume expansion during data analysis using the volume expansion data for CO_2-expanded acetonitrile from Lazzaroni et al.[36]

The excessive amount of the PTAD dienophile (100:1 of PTAD:anthracene) resulted in pseudo-first order kinetics in anthracene concentration. As a result, the concentration of PTAD could be assumed to remain essentially constant over the course of the experiment, and the second-order rate constant is calculated by the rate of disappearance of anthracene and the concentration of PTAD. Equilibrium pressure was typically reached within 5 minutes from the time anthracene was introduced, and only data recorded after that time were used in determining the rate constant. Individual kinetic experiments were carried out for a minimum of two half-lives (usually 1-3 hours).

Linear plots of anthracene fluorescence (and thus, concentration) versus time confirmed pseudo-first order conditions.

Results and Discussion

Solvatochromic parameters

Reichardt's $E_T(30)$ parameter includes both dipolarity and hydrogen bond donor acidity.[23, 24] The $E_T(30)$ value, measured in kcal/mol, is determined by measuring the solvent-dependent transition energy for the intramolecular charge transfer of the Dimroth-Reichardt betaine dye using the following equation:

$$E_T(30) = \frac{hcN_A}{\lambda_{\max}} \qquad \text{Equation 2-3}$$

where h is Planck's constant, c is the speed of light, N_A is Avogadro's number, and λ_{max} is the wavelength of maximum absorption of the probe molecule (measured in nm).

Figure 2.3 shows the $E_T(30)$ of GX-acetonitrile as a function of composition determined in these experiments. Preferential solvation of the probe by acetonitrile (i.e. the solvent shell surrounding the probe contains mostly acetonitrile molecules) results in only a small change in $E_T(30)$ up to $x_{CO2} = 0.85$. Beyond this concentration of CO_2, the solubility of the probe molecule was below the UV detection limit. Literature data in pure CO_2 suggests a sharp decrease in $E_T(30)$ at $CO_2 > 0.85$.[37]

The Kamlet-Taft π^* parameter measures the relative solvent dipolarity and polarizability by quantifying dipole-dipole or dipole-induced dipole interactions between

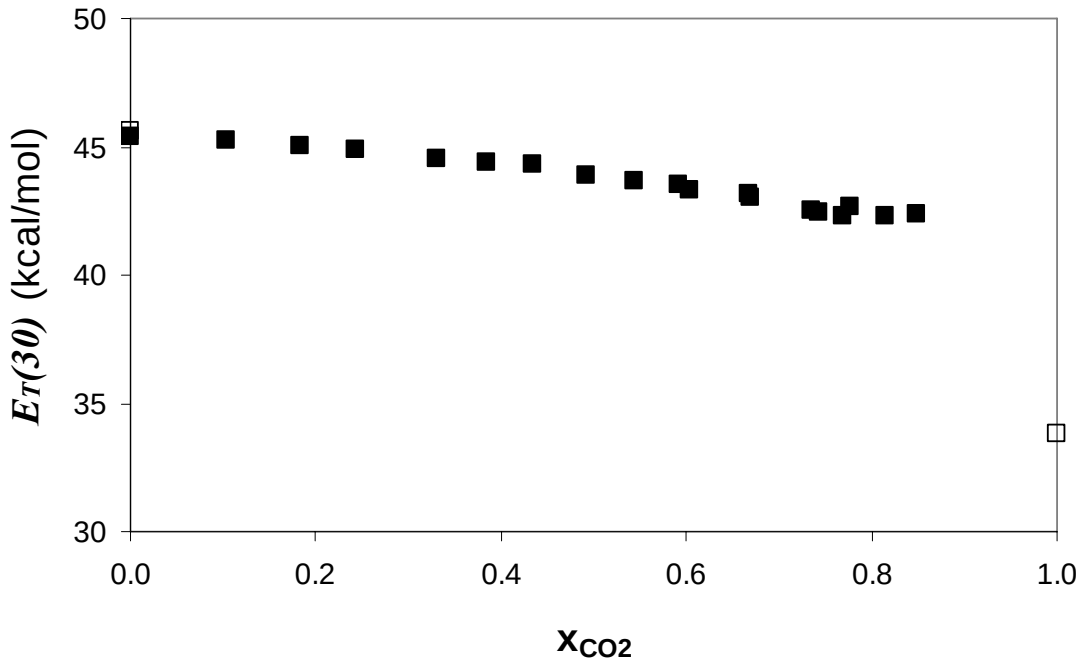

Figure 2.3: $E_T(30)$ for CO_2-expanded acetonitrile as a function of composition. (□) literature values[17, 37] (■) our experimental values.

the solute and the solvent.[16] We have used *p*-nitroanisole as the π^* indicator molecule for this work, although *N*,*N*-dimethyl-*p*-nitroaniline is also commonly used.[10] The wavenumber of the maximum absorbance (ν) of the indicator is determined spectroscopically; then the π^* value is calculated with respect to the reference solvents cylcohexane ($\pi^* = 0$) and DMSO ($\pi^* = 1$).[16, 25] Our measurements for the wavenumbers of *p*-nitroanisole in cyclohexane ($\nu = 34075$ cm^{-1}) and DMSO ($\nu = 31829$ cm^{-1}) were consistent with literature data to ±0.5%.[10] The π^* value (see Figure 2.4) shows a smooth, gradual decrease from its value in pure acetonitrile up to $x_{CO2} = 0.85$. The value then drops dramatically to the pure CO_2 value. As may be expected, this trend is similar to that of Wyatt et al. reported in gas-expanded acetone.[10]

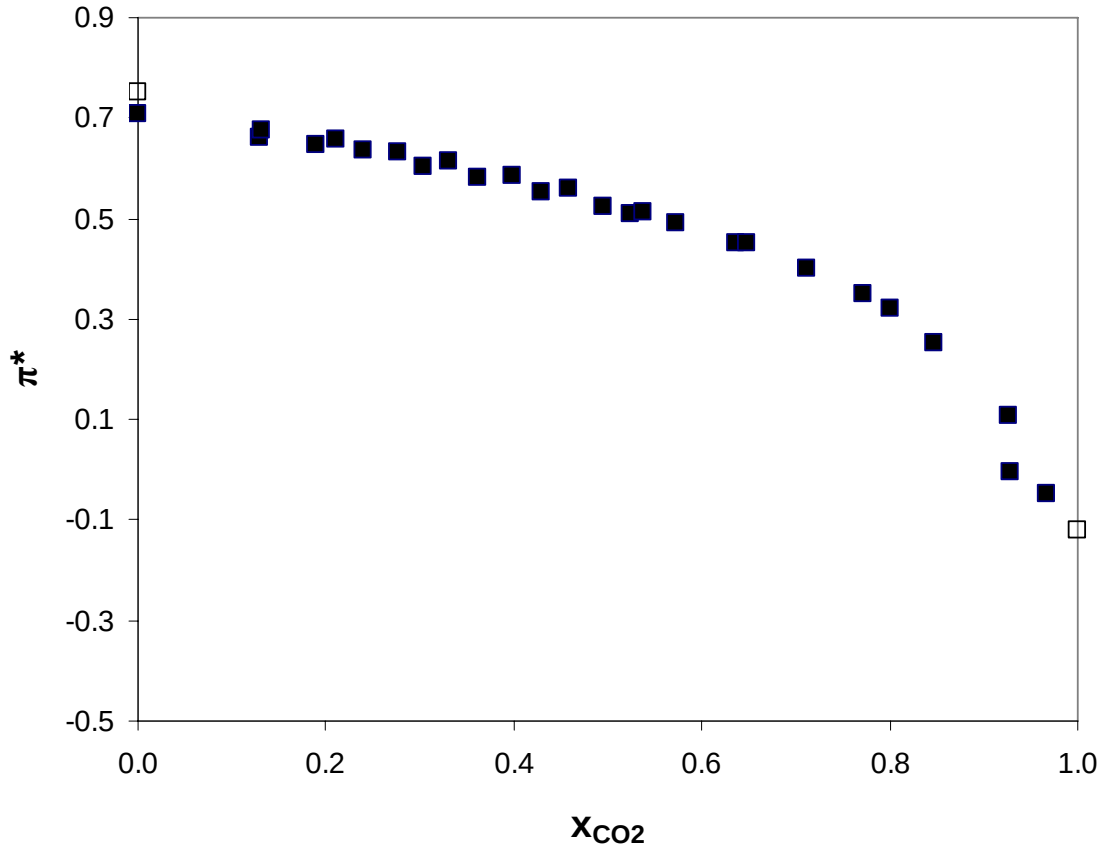

Figure 2.4: π^* for CO_2-expanded acetonitrile as a function of composition. (□) literature values[17, 48] (■) our experimental values.

The Kamlet-Taft α parameter quantifies the ability of the solvent to donate a hydrogen bond. Our calculation of α is based on experimental measurements of π^* and $E_T(30)$ using the procedure described by Marcus:[17]

$$\alpha = 0.0649[E_T(30) - E_T(30)_{ACN}] - 0.72[\pi^* - \pi^*_{ACN}] + 0.19 \qquad \text{Equation 2-4}$$

where $E_T(30)_{ACN}$ and π^*_{ACN} represent the values of those solvatochromic parameters in pure acetonitrile.

As with $E_T(30)$, α is relatively constant near the pure acetonitrile value up to x_{CO2} = 0.60, indicating preferential solvation (see Figure 2.5). Beyond x_{CO2} = 0.80, the value increases sharply towards the pure CO_2 value.

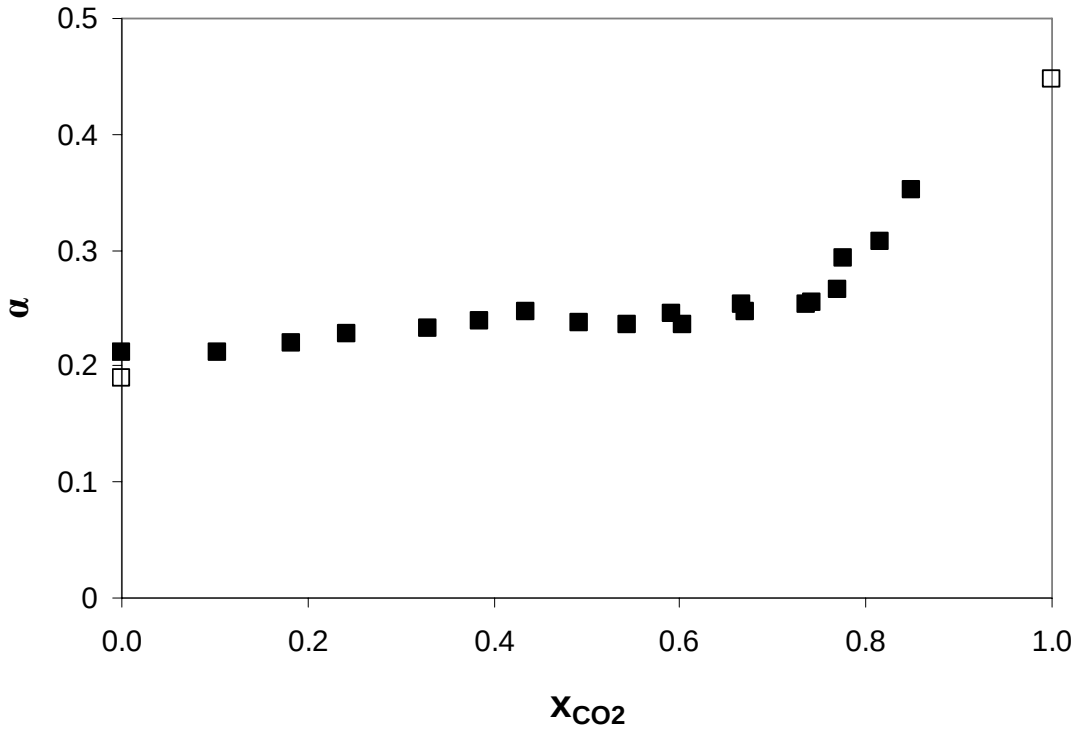

Figure 2.5: α for CO_2-expanded acetonitrile as a function of composition. (□) literature values[17, 37] (■) our experimental values.

The Kamlet-Taft β parameter is determined through a comparative method using a non-hydrogen-bond acceptor probe, *p*-nitroanisole (the π^* probe), and a corresponding hydrogen-bond acceptor probe, *p*-nitrophenol.[10, 19-21, 38] The β parameter for a given solvent is calculated based on the displacement of that solvent from the reference line for the probe pair. The reference line for the probe pair used in this work is:[21]

$$\nu(2)_{calc} = 0.901\nu(1) + 4160 \qquad \text{Equation 2-5}$$

where $\nu(1)$ represents the wavenumber (cm^{-1}) of maximum absorbance for *p*-nitroanisole in the solvent of interest, and $\nu(2)_{calc}$ represents the wavenumber of maximum absorbance for *p*-nitrophenol calculated based the reference line.

The displacement for the solvent of interest from this reference line is then calculated by:[21]

$$-\Delta\Delta\nu(2-1) = \frac{\nu(2)_{calc} - \nu(2)_{obs}}{1000} \qquad \text{Equation 2-6}$$

In this equation, $\nu(2)_{obs}$ is the experimentally-measured wavenumber of maximum absorbance for *p*-nitrophenol in the solvent of interest. The value $-\Delta\Delta\nu(2-1)$ is the displacement from the reference line.

Finally, β is calculated based on $-\Delta\Delta\nu(2-1)$:[21]

$$\beta = \frac{-\Delta\Delta\nu(2-1)}{(2.80)(0.825)} \qquad \text{Equation 2-7}$$

The β scale is normalized to a value of 1 for hexamethylphosphoramide and 0 for cyclohexane.[10]

The most peculiar results in our solvatochromic studies came from the β parameter, as shown in Figure 2.6. The data show a moderate but significant increase in β up to $x_{CO2} = 0.90$ followed by a precipitous decrease at higher CO_2 compositions. These data are the result of multiple cell loadings and the trends are confirmed over multiple experimental runs.

A closer look at the solvent structure reveals a possible explanation for the unusual β behavior: the extended dipole of the acetonitrile-CO_2 complex (see Figure 2.7). If acetonitrile and CO_2 align in a "T" formation with the CO_2 carbon adjacent to the nitrile group of acetonitrile, the resulting dipole is longer, and stronger, than the

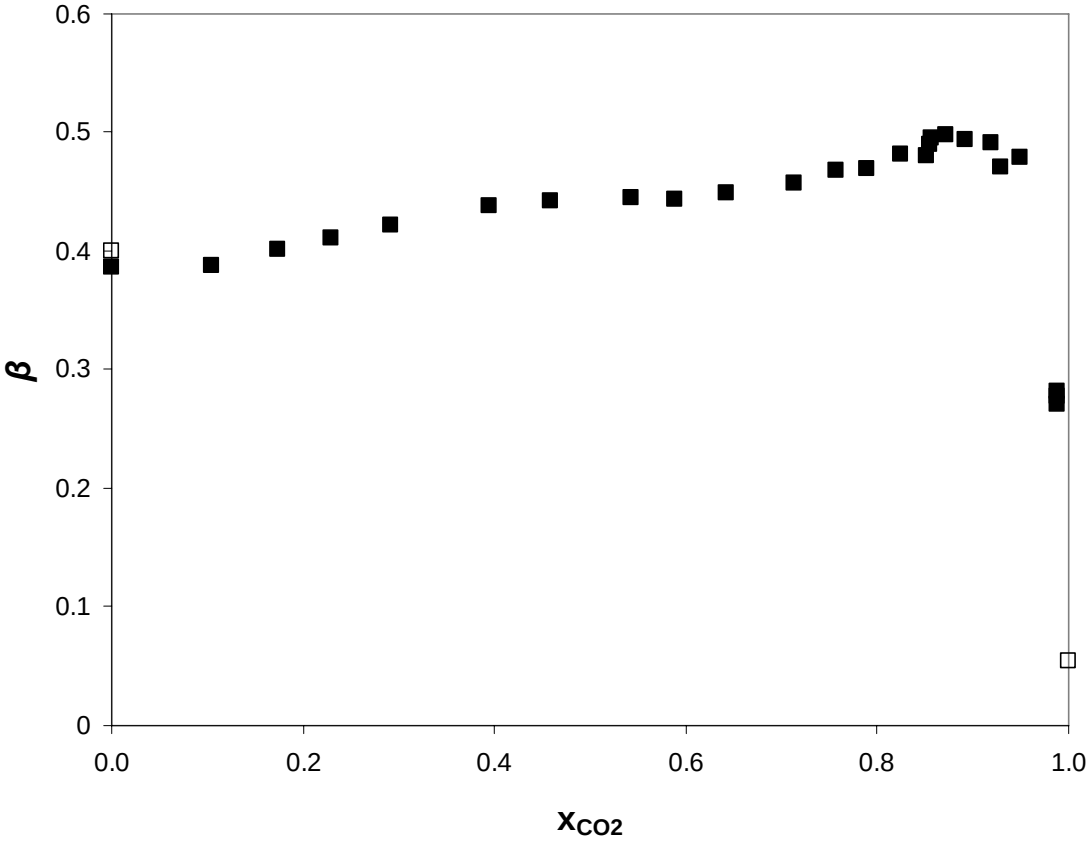

Figure 2.6: β for CO_2-expanded acetonitrile as a function of composition. (□) literature values[17, 48] (■) our experimental values.

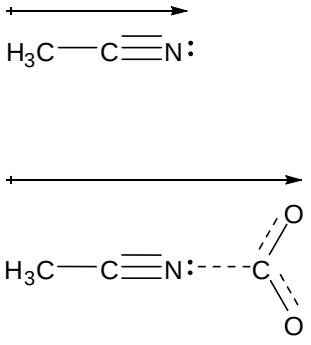

Figure 2.7: Extended dipole in the acetonitrile-CO_2 complex.

acetonitrile dipole alone. Williams et al. have shown through symmetry-adapted perturbation theory computations that this configuration is energetically favorable among the geometries they considered, and thus it is likely to occur in solutions of acetonitrile and CO_2.[39]

In addition to creating a stronger dipole moment, the acetonitrile-CO_2 complex causes the oxygen atoms of CO_2 to become more electronegative and more capable of accepting hydrogen bonds. Although these interactions may be important in explaining the β results, they do not necessarily contradict our π^* results that showed a decrease in polarity when adding CO_2. The acetonitrile-CO_2 complex described here needs to be present only in small amounts to have a large effect on α and β, while having a minimal impact on the polarity. We attempted to obtain additional evidence to support the formation of this complex via IR spectroscopy, but the data suggest that the complex forms only in small quantities if at all.[40]

Kinetic results

Our data for pure acetonitrile (see Figure 2.8) are consistent with literature data for this reaction.[28, 30] Although Diels-Alder reactions often accelerate in polar solvents, our data show an increase in rate constant as CO_2 (a nonpolar solvent) is added.[41] A careful review of literature shows that the reaction of PTAD and anthracene does not follow the trend of other Diels-Alder reactions.[28, 29] Indeed, Burrage et al. showed that the opposite trend occurs; i.e., the rate constant decreases going from benzene ($E_T(30)$ = 34.3 kcal/mol) to dioxane ($E_T(30)$ = 36.0 kcal/mol) to ethyl acetate ($E_T(30)$ = 38.1 kcal/mol).[29] Konovalov et al. proposed that electron donor-acceptor interactions are

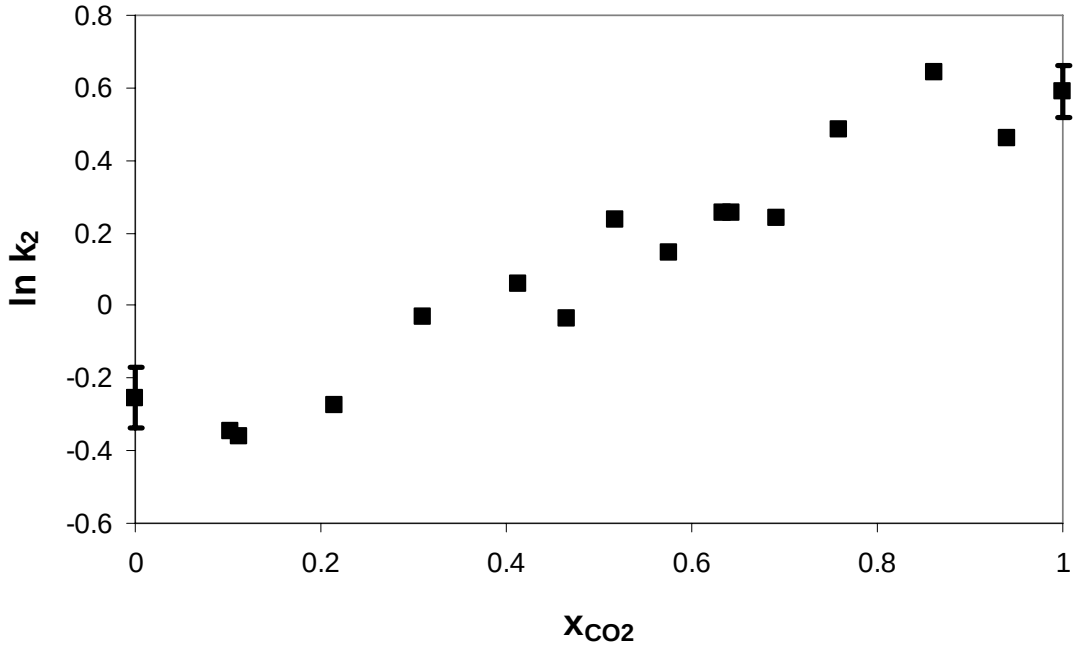

Figure 2.8: Diels-Alder rate constant for CO_2-expanded acetonitrile as a function of composition.

more important than polarity for this reaction and showed that the activation enthalpy of the reaction is lowered in electron-accepting solvents due to the electron-donating nature of the transition state of the reaction.[28]

One possible explanation of our results is that CO_2 is acting as a Lewis acid to accelerate the reaction. We speculate that a Lewis-acid interaction at the carbonyl oxygens of the PTAD (see Figure 2.9) would destabilize the azo-bond, increasing the reactivity of the dienophile towards the diene. This explanation is supported by our β measurements, which show an increase as CO_2 is added to the system. Burrage et al. proposed that, while PTAD is an electron acceptor, the transition state of the reaction between PTAD and anthracene becomes electron-donating.[29] This transition-state

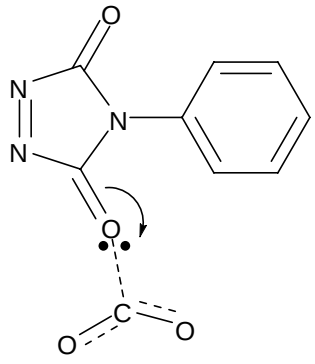

Figure 2.9: Proposed mechanism of Lewis-acid catalysis by CO_2 on PTAD.

stabilization by electron withdrawing solvents has been found in other similar Diels-Alder reactions as well.[42, 43] We hypothesize that the electron-donating transition state is stabilized in the higher-β (more electron-accepting) solvent as CO_2 is added.

At high CO_2 compositions, solute clustering may occur which further accelerates the reaction.[12, 44] Qian et al. measured the rate constant for the similar Diels-Alder reaction of *N*-ethylmaleimide and 9-hydroxymethylanthracene in supercritical CO_2 and found a substantial rate increase relative to organic solvents.[45] They offered solvophobic interactions, which force clustering of reactants within the solvent, as the cause of this acceleration. Similar solvophobic acceleration of Diels-Alder reactions has been reported in water and fluorinated solvents.[46, 47]

LSER results

We used multiple linear regression to determine the coefficients in the LSER model. Solvatochromic parameter data was regressed using polynomial fits (correlation coefficient >0.98 for all curves) in order to estimate accurately parameter values for the entire solvent composition range. For each experimental data point in the kinetic rate constant versus GXL composition curve, we calculated the solvatochromic parameters

using the polynomial fits of the experimental solvatochromic parameter data at that composition. The kinetic data were then regressed against the solvatochromic data to determine the values of the LSER coeffecients. The resulting equation is (with 90% confidence intervals for each coefficient in parentheses):

$$\ln k_2 = 1.90(\pm 1.08) - 2.62(\pm 0.76)\pi^* - 4.68(\pm 2.53)\alpha + 1.58(\pm 0.73)\beta \qquad \text{Equation 2-8}$$

The correlation coefficient for our LSER model was high ($r^2 = 0.96$), and as shown in Figure 2.10, the correlation accurately represents the data trend over the entire composition range. The rate of the reaction is increased as π^* decreases, which is consistent with literature data as stated above. α and β have opposing effects, as might be expected. This trend suggests that perhaps electron donor-acceptor complexes between CO_2 and the transition state of the reaction, including Lewis acid-base interactions, help to stabilize the transition state relative to the reactants. This hypothesis is consistent with our solvatochromic data as well as the LSER model.

We were unable to predict accurately the kinetic data of Konovalov et al. for the reaction of PTAD and anthracene in organic solvents using our LSER equation.[28] While we agree with the overall conclusions of the paper, a more thorough review of the literature leads us to speculate that PTAD may have decomposed in some of the solvents in their work. PTAD instability has been reported in acids and bases, alcohols, water.[31-33] We have also observed color changes in solutions of PTAD in tetrahydrofuran, ethyl acetate, and chloroform.

The kinetic data of Konovalov et al. were determined by UV measurements of PTAD intensity. This technique is susceptible to error if PTAD decomposition occurs

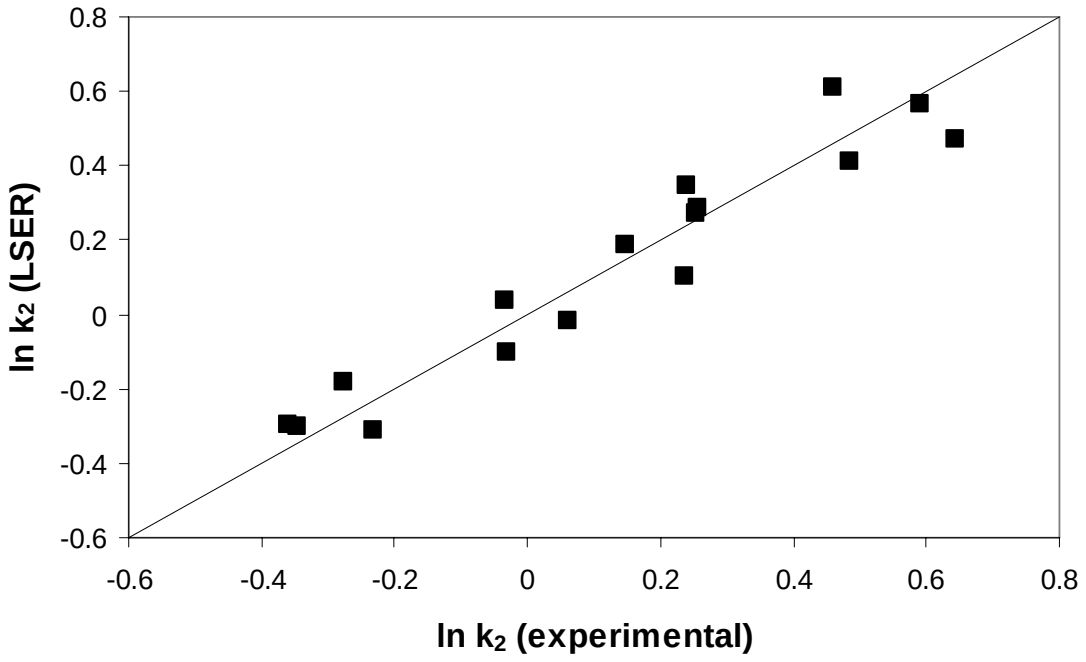

Figure 2.10: LSER-predicted versus experimental values of rate constant. (■) LSER prediction (–) predicted value equals experimental value line.

due to the solvent rather than the diene. Since our method is dependent on anthracene fluorescence, it is more robust and reliable. PTAD decomposition, if it occurred in our experiments, would slow down rather than accelerate the observed reaction rate. The repeatability of our kinetic data in pure acetonitrile and pure CO_2 further supports our analytical technique. A calorimetric study mirroring that of Konovalov and coworkers would provide additional thermodynamic data on this reaction in gas-expanded acetonitrile.[28] Such a study would allow comparison between the enthalpy of solvation of the reactants (particularly PTAD) and the transition state at the various solvent compositions of gas-expanded acetonitrile used in this work.

Conclusions

We have combined the results of kinetic and solvatochromic studies to develop a better understanding of the intermolecular interactions in the cybotactic region of CO_2-expanded acetonitrile. Our results suggest the formation of an extended-dipole complex between CO_2 and acetonitrile that affects hydrogen bonding between the solvent and solutes. In addition, we speculate that CO_2 acts as a Lewis acid to accelerate the Diels-Alder reaction between PTAD and anthracene.

This work demonstrates the effectiveness of a multi-parameter approach to model the kinetics of a reaction in CO_2-expanded acetonitrile. The linear solvation energy relationship employed here predicts accurately the kinetic data while providing quantitative insight into the specific molecular interactions taking place. The results of this work can be used to guide future applications of gas-expanded liquids as reaction solvents.

References

1. Eckert, C. A.; Liotta, C. L.; Bush, D.; Brown, J. S.; Hallett, J. P., Sustainable reactions in tunable solvents. *J. Phys. Chem. B* **2004,** *108*, 18108.

2. Sala, S.; Tassaing, T.; Ventosa, N.; Danten, Y.; Besnard, M.; Veciana, J., Molecular insight, through IR spectroscopy, on solvating phenomena occurring in CO_2-expanded solutions. *ChemPhysChem* **2004,** *5*, 243.

3. Wei, M.; Musie, G. T.; Busch, D. H.; Subramaniam, B., CO_2-expanded solvents: unique and versatile media for performing homogeneous catalytic oxidations. *J. Am. Chem. Soc.* **2002,** *124* (11), 2513.

4. Anand, M.; McLeod, M. C.; Bell, P. W.; Roberts, C. B., Tunable solvation effects on the size-selective fractionation of metal nanoparticles in CO_2 gas-expanded solvents. *J. Phys. Chem. B* **2005,** *109*, 22852.

5. Eckert, C. A.; Bush, D.; Brown, J. S.; Liotta, C. L., Tuning solvents for sustainable technology. *Ind. Eng. Chem. Res.* **2000,** *39*, 4615.

6. Song, I.; Spuller, M.; Levitin, G.; Hess, D. W., Photoresist and residue removal using gas-expanded liquids. *J. Electrochem. Soc.* **2006,** *153* (4), G314.

7. Jin, H.; Subramaniam, B., Homogeneous catalytic hydroformylation of 1-octene in CO_2-expanded solvent media. *Chem. Eng. Sci.* **2004,** *59*, 4887.

8. West, K. N.; Wheeler, C.; McCarney, J. P.; Griffith, K. N.; Bush, D.; Liotta, C. L.; Eckert, C. A., In situ formation of alkylcarbonic acids with CO_2. *J. Phys. Chem. A* **2001,** *105*, 3947.

9. Sala, S.; Ventosa, N.; Tassaing, T.; Cano, M.; Danten, Y.; Besnard, M.; Veciana, J., Synergistic enhancement of the solubility of hexamethylenetetramine in subcritical CO_2-ethanol mixtures studied by infrared spectroscopy. *ChemPhysChem* **2005,** *6*, 587.

10. Wyatt, V. T.; Bush, D.; Lu, J.; Hallett, J. P.; Liotta, C. L.; Eckert, C. A., Determination of solvatochromic solvent parameters for the characterization of gas-expanded liquids. *J. Supercritical Fluids* **2005,** *36*, 16.

11. Kelley, S. P.; Lemert, R. M., Solvatochromic characterization of the liquid phase in liquid-supercritical CO_2 mixtures. *AIChE J.* **1996,** *42* (7), 2047.

12. Kim, S.; Johnston, K. P., Clustering in supercritical fluid mixtures. *AIChE J.* **1987,** *33* (10), 1603.

13. Eckert, C. A.; Knutson, B. L.; Debenedetti, P. G., Supercritical fluids as solvents for chemical and materials processing. *Nature* **1996,** *383*, 313.

14. Knutson, B. L.; Tomasko, D. L.; Eckert, C. A.; Debenedetti, P. G.; Chialvo, A. A., Local density augmentation in supercritical solutions. A comparison between fluorescence spectroscopy and molecular dynamics results. In *Supercritical Fluid Technology*, Bright, F. V.; McNally, M. E. P., Eds. ACS Symposium Series; American Chemical Society: Washington, DC, 1992; Vol. 488, pp 60-72.

15. Ting, S. S. T.; Tomasko, D. L.; Macnaughton, S. J.; Foster, N. R., Chemical-Physical Interpretation of Cosolvent Effects in Supercritical

Fluids. *Ind. Eng. Chem. Res.* **1993,** *32*, 1482.

16. Kamlet, M. J.; Abboud, J. L.; Taft, R. W., The solvatochromic comparison method. 6. The p* scale of solvent polarities. *J. Am. Chem. Soc.* **1977,** *99* (18), 6027.

17. Marcus, Y., The properties of organic liquids that are relevant to their use as solvating solvents. *Chem. Soc. Rev.* **1993**, 409.

18. Taft, R. W.; Kamlet, M. J., The solvatochromic comparison method. 2. The a-scale of solvent hydrogen-bond donor (HBD) acidities. *J. Am. Chem. Soc.* **1976,** *98* (10), 2886.

19. Laurence, C.; Nicolet, P.; Helbert, M., Polarity and basicity of solvents Part 2. Solvatochromic hydrogen-bonding shifts as basicity parameters. *J. Chem. Soc. Perkin Trans. II* **1986**, 1081.

20. Nicolet, P.; Laurence, C., Polarity and basicity of solvents. Part 1. A thermosolvatochromic comparison method. *J. Chem. Soc. Perkin Trans. II* **1986**, 1071.

21. Kamlet, M. J.; Taft, R. W., The solvatochromic comparison method. I. The b-scale of solvent hydrogen-bond acceptor (HBA) basicities. *J. Am. Chem. Soc.* **1976,** *98* (2), 377.

22. Mellein, B. R.; Aki, S. N. V. K.; Ladewski, R. L.; Brennecke, J. F., Solvatochromic studies of ionic liquid/organic mixtures. *J. Phys. Chem. B* **2007,** *111* 131.

23. Lu, J.; Brown, J. S.; Boughner, E. C.; Liotta, C. L.; Eckert, C. A., Solvatochromic characterization of near-critical water as a benign reaction medium. *Ind. Eng. Chem. Res.* **2002,** *41*, 2835.

24. Reichardt, C., Solvatochromic dyes as solvent polarity indicators. *Chem. Rev.* **1994,** *94*, 2319.

25. Lu, J.; Liotta, C. L.; Eckert, C. A., Spectroscopically probing microscopic solvent properties of room-temperature ionic liquids with the addition of carbon dioxide. *J. Phys. Chem. A* **2003,** *107*, 3995.

26. Sigman, M. E.; Lindley, S. M.; Leffler, J. E., Supercritical carbon dioxide: Behavior of p* and b solvatochromic indicators in media of different densities. *J. Am. Chem. Soc.* **1985,** *107*, 1471.

27. Tada, E. B.; Novaki, L. P.; El Seoud, O. A., Solvatochromism in pure and binary solvent mixtures: effects of the molecular structure of the zwitterionic probe. *J. Phys. Org. Chem.* **2000,** *13*, 679.

28. Konovalov, A. I.; Breus, I. P.; Sharagin, I. A.; Kiselev, V. D., Study of solvation effects in Diels-Alder reactions of 4-phenyl-1,2,4-triazoline-3,5-dione with anthracene

and trans,trans-1,4-diphenyl-1,3-butadiene. *Zhurnal organicheskoi khimii* **1979,** *15* (2), 361.

29. Burrage, M. E.; Cookson, R. C.; Gupte, S. S.; Stevens, I. D. R., Substituent and solvent effects on the Diels-Alder reactions of triazoline diones. *J. Chem. Soc., Perkin Trans. II* **1975**, 1325.

30. Thompson, R. L.; Glaser, R.; Bush, D.; Liotta, C. L.; Eckert, C. A., Rate variations of a hetero-Diels-Alder reaction in supercritical fluid CO_2. *Ind. Eng. Chem. Res.* **1999,** *38*, 4220.

31. Cookson, R. C.; Gilani, S. S. H.; Stevens, I. D. R., 4-Phenyl-1,2,4-triazolin-3,5-dione: A powerful dienophile. *Tetrahedron Letters* **1962,** (14), 615.

32. Dao, L. H.; Mackay, D., Duality of pathways in the reaction of *N*-phenyltriazolinedione with alcohols. *J. Chem. Soc. Chem. Comm.* **1976**, 326.

33. Izydore, R. A.; Johnson, H. E.; Horton, R. T., Decomposition reactions of a cis-diacyl diimide. 4-Phenyl-1,2,4-triazoline-3,5-dione. *J. Org. Chem.* **1985,** *50*, 4589.

34. Cookson, R. C.; Gilani, S. S. H.; Stevens, D. R., Diels-Alder reactions of 4-phenyl-1,2,4-triazoline-3,5-dione. *J. Chem. Soc. C, Org.* **1967**, 1905.

35. Lu, J.; Brown, J. S.; Liotta, C. L.; Eckert, C. A., Polarity and hydrogen-bonding of ambient to near-critical water: Kamlet-Taft solvent parameters. *Chem. Commun.* **2001**, 665.

36. Lazzaroni, M. J.; Bush, D.; Brown, J. S.; Eckert, C. A., High-pressure vapor-liquid equilbria of some carbon dioxide + organic binary systems. *J. Chem. Eng. Data* **2005,** *50*, 60.

37. Hyatt, J. A., Liquid and Supercritical Carbon Dioxide as Organic Solvents. *J. Org. Chem.* **1984,** *49*, 5097.

38. Lagalante, A. F.; Spadi, M.; Bruno, T. J., Kamlet-Taft solvatochromic parameters of eight alkanolamines. *J. Chem. Eng. Data* **2000,** *45*, 382.

39. Williams, H. L.; Rice, B. M.; Chabalowski, C. F., Investigation of the CH_3CN-CO_2 potential energy surface using symmetry-adapted perturbation theory. *J. Phys. Chem. A* **1998,** *102*, 6981.

40. Kazarian, S. Imperial College, London, United Kingdom. Personal Communication, 2007.

41. McCabe, J. R.; Eckert, C. A., High-pressure kinetic studies of solvent and substituent effects on Diels-Alder reactions. *Ind. Eng. Chem., Fundam.* **1974,** *Vol. 13* (No. 3), 168.

42. Cativiela, C.; Garcia, J. I.; Mayoral, J. A.; Salvatella, L., Modelling of solvent effects on the Diels-Alder reaction. *Chem. Soc. Rev.* **1996**, 209.

43. Atherton, J. C. C.; Jones, S., Diels-Alder reactions of anthracene, 9-substituted anthracenes and 9,10-disubstituted anthracenes. *Tetrahedron* **2003,** *59*, 9039.

44. Wang, B.; Han, B.; Jiang, T.; Zhang, Z.; Xie, Y.; Li, W.; Wu, W., Enhancing the rate of the Diels-Alder reaction using CO_2 + ethanol and CO_2 + *n*-hexane mixed solvents of different phase regions. *J. Phys. Chem. B* **2005,** *109*, 24203.

45. Qian, J.; Timko, M. T.; Allen, A. J.; Russell, C. J.; Winnik, B.; Buckley, B.; Steinfeld, J. I.; Tester, J. W., Solvophobic acceleration of Diels-Alder reactions in supercritical carbon dioxide. *J. Am. Chem. Soc.* **2004,** *126*, 5465.

46. Myers, K. E.; Kumar, K., Fluorophobic acceleration of Diels-Alder reactions. *J. Am. Chem. Soc.* **2000,** *122*, 12025.

47. Rideout, D. C.; Breslow, R., Hydrophobic acceleration of Diels-Alder reactions. *J. Am. Chem. Soc.* **1980,** *102*, 7816.

48. Bulgarevich, D. S.; Sako, T.; Sugeta, T.; Otake, K.; Takebayashi, Y.; Kamizawa, C.; Horikawa, Y.; Kato, M., The role of general and hydrogen-bonding interactions in the solvation processes of organic compounds by supercritical CO_2/n-alcohol mixtures. *Ind. Eng. Chem. Res.* **2002,** *41*, 2074.

CHAPTER III

LOCAL POLARITY IN CO_2-EXPANDED ACETONITRILE: A NUCLEOPHILIC SUBSTITUTION REACTION AND SOLVATOCHROMIC PROBES

Introduction

Gas-expanded liquids (GXLs) are an important class of alternative solvents that have received a great deal of attention in the last 20 years, as evidenced by a recent review by Jessop & Subramaniam.[1] Several techniques for particle and nanoparticle formation have been developed that exploit the tunable nature of GXLs to control the particle quality and size distribution.[2-7] GXLs also have been used for photoresist removal in microelectronics processing.[8] Another significant application of GXLs is as a reaction solvent for homogeneous and heterogeneous catalysis.[9-14] Characteristic to many of these processes is the utilization of CO_2 to alter the polarity of the solvent and facilitate a change in the phase behavior of the system.

Previous work with cosolvent-modified supercritical CO_2, as well as gas-expanded liquids has suggested an important phenomenon in these solvents: differences between the local and bulk properties of the solvent. Preferential solvation of solute molecules by one of the components in a mixed solvent can result in behavior not adequately described in terms of bulk solvent properties. The differences between bulk and local properties have been demonstrated by spectroscopic, solubility, and kinetic measurements in supercritical fluids and GXLs.[15-18]

Knowledge of how these properties change for various solvents as a function of CO_2 concentration can lead to opportunities in design of reactions and separation process

development. In this work, we examine and compare several measures of solvent polarity in CO_2-expanded acetonitrile. Our purpose in this work is to determine how both the bulk and local polarity change as a function of solvent composition to enable more effective industrial implementation of these unique tunable solvents.

We have examined several probes as indicators of either local or bulk polarity in CO_2 expanded acetonitrile. As in our previous study, polar aprotic acetonitrile was chosen as the organic solvent to provide a wide property range for the resulting CO_2-expanded liquid.[19]

Solvatochromic probes

Solvatochromic probes are often used to quantify solvent properties for pure fluids and fluid mixtures.[20-28] We focus in this work on two well-established solvatochromic probes of polarity and/or polarizability: the Kamlet-Taft π^* parameter and Kosower's Z (see Figure 3.1).[22, 29]

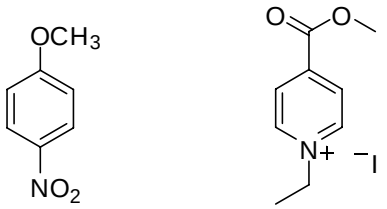

(1) (2)

Figure 3.1: Solvatochromic probes: (1) *p*-nitroanisole (2) 1-ethyl-4-carbomethoxypyridinium iodide.

The Kamlet-Taft dipolarity/polarizablity parameter, π^*, provides a comprehensive measure of a solvent's ability to stabilize a solute molecule based on dielectric effects.[30-32] Because π^* is a measure of a probe molecule's response to its surroundings upon excitation, it is a quantitative index of the solvent's dipolarity/polarizability in the cybotactic region about the ground state of the probe molecule.[31] The technique has been

used extensively for measuring the polarity of pure solvents, ambient liquid mixtures and CO_2-expanded solvents.[28, 30, 33, 34] The experimental determination of individual π^* values are typically obtained from the shifts of the electronic absorption maxima of designated spectroscopic indicators.[30, 32] We applied previously measured π^* values based on *p*-nitroanisole as the probe molecule to correlate the kinetic behavior of the S_N2 reaction.

Kosower developed a polarity parameter called the *Z*-value based on his findings that the charge-transfer light absorption band of 1-alkylpyridinium iodides is very sensitive to the polarity of a solvent.[29, 35] The *Z*-value is defined as the transition energy (E_T) for the longest wavelength absorption band observed for 1-ethyl-4-carbomethoxypyridinium iodide in that solvent,[35] similar to solvatochromic scales such as $E_T(30)$, Nile Red, Crystal Violet, etc.[36] Governing equations are found in the experimental procedure section. As with π^*, a higher *Z* indicates a higher polarity.[29, 35]

Menschutkin reaction

The Menschutkin reaction is a nucleophilic substitution reaction with an S_N2 mechanism between a nitrogen base, typically a tertiary amine, and a sulfonate or an alkyl halide to form a quaternary ammonium salt in which the formal hybridization of the nitrogen atom is sp^2 or sp^3.[37, 38] This class of reactions is a good probe of polarity because its transition state is much more polar than the reactants; thus the reaction kinetics depend strongly on the polarity of the surrounding medium. The Menschutkin reactions of different substrates have been studied in a variety of media including organic solvents, ionic liquids, and gases.[39-41]

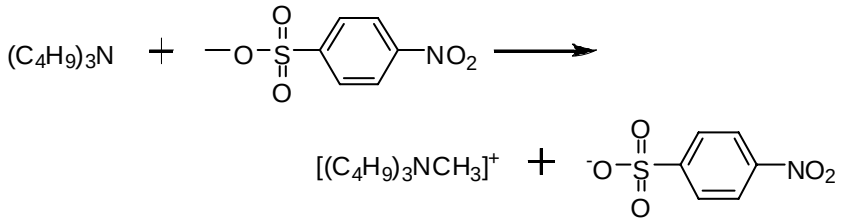

Figure 3.2: S_N2 reaction of TBA and MNBS.

In this study we have chosen the reaction of tri-butylamine (TBA) with methyl *p*-nitrobenzenesulfonate (MNBS), as illustrated in Figure 3.2. This reaction is well-characterized and has been used to study the polarity and nucleophilicity of ionic liquids.[39, 40] Importantly, MNBS has a λ_{max} at 253 nm while the product, the *p*-nitrobenzenesulfonate ion, has a λ_{max} at 275 nm. Because the two peaks are sufficiently separated, the reaction can be monitored *in situ* via UV-Vis spectroscopy. The corresponding polar transition state, which plays a key role in probing the polarity in the cybotactic region, is shown in Figure 3.3. For each reaction it was possible to record absorbance values at 253 nm and 275 nm at known time intervals and use them to determine the rate of the reaction. An isosbestic point is always observed.

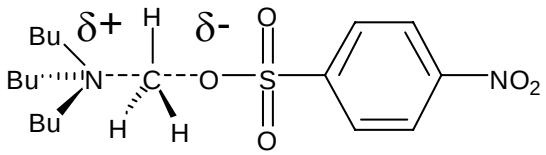

Figure 3.3: Charge-separated transition state of the reaction of TBA and MNBS.

Experimental

Materials

Carbon dioxide was purchased from Airgas and filtered before use. Tributylamine (ReagentPlus, ≥98.5%), 1-ethyl-4-carbomethoxypyridinium iodide (97%) and acetonitrile

(HPLC, ≥99.9%) were purchased from Sigma-Aldrich. Methyl *p*-nitrobenzenesulfonate (99%) was purchased from Acros Organics. All solvents were used as received. No assays for water content were performed.

Apparatus

A stainless steel vessel with two sapphire windows (6.4-mm thick) was constructed for *in-situ* high pressure UV-Vis spectroscopy. The windows were sealed with Teflon gaskets capable of withstanding pressures over 250 bar. The cell has a path length of 2.2 cm and an internal volume of 13 ml. Temperature was controlled with a refrigerated constant temperature flow bath (Thermo Electron Corporation, Neslab RTE7) with a mixture of ethylene glycol and water as the heat transfer fluid and monitored with a thermocouple and readout (Omega). The temperature variation was maintained within ±0.1°C of the set point. Pressure was monitored by a pressure transducer and readout (Druck) with an uncertainty of ±1 psi. A magnetic spin bar and motor (H+P Labortechnik, Variomag Telemodul 20C) constantly agitated the cell contents to facilitate equilibrium. Temperature and pressure gauges were calibrated to ensure their accuracy in these experiments. CO_2 was metered into the vessel using a syringe pump (ISCO, 260D). All measurements were performed on a Hewlett-Packard 8453 UV/vis spectrophotometer (1 nm resolution and ±0.2 nm wavelength accuracy). Both kinetic and solvatochromic experiments were performed in the same apparatus.

Procedure

For kinetic experiments, we prepared stock solutions of TBA and MNBS in acetonitrile. We loaded the cell with 5 mL of 6×10^{-4} mol/L solution of TBA in acetonitrile and heated the cell to 40ºC. Then we added 50 μL of 6×10^{-3} mol/L solution

of MNBS in acetonitrile, sealed the cell, and added CO_2 to the desired pressure (i.e. x_{CO2}). We maintained at least a 10:1 excess of TBA to MNBS in all experiments to allow pseudo-first-order kinetic analysis. We corrected the concentrations of the reactants for solvent volume expansion using phase behavior data from the literature for CO_2-expanded acetonitrile.[42] We monitored the reaction at given time intervals until both product and reactant peaks remained constant for at least one half-life. The experiment durations range from 6 hours to more than two weeks, depending on the solvent composition.

Peak intensities at 253 nm and 275 nm were recorded and plotted as a function of time. Data were treated by a least-squares fitting procedure using a user-defined function in OriginLab Software Package (Version 7.5).[43] Equations 1 and 2 are fit to the data simultaneously in order to determine the pseudo-first-order rate constant, k_{obs}. The model is based on a typical "A to B" reaction where A_0 is the initial amount of substrate and B_∞ is the final amount of product. A and B denote the amounts of reactant and product, respectively, at a given time, t. The constants C_1 and C_2 are required to correct for the fact that the UV absorbance is not zero when the concentration of A or B is equal to zero. The resulting k_{obs} value is divided by the initial concentration of TBA to calculate a second-order rate constant, k_2.

$$A = A_0 e^{-k_{obs}t} + C_1 \qquad \text{Equation 3-1}$$

$$B = B_\infty (1 - e^{-k_{obs}t}) + C_2 \qquad \text{Equation 3-2}$$

In our solvatochromic measurements, we prepared concentrated stock solutions of the solvatochromic probes in acetonitrile. We then diluted a known volume of the stock solution into acetonitrile to attain a UV-Vis response within the range of the detector.

After sealing the cell, we added CO_2 to the desired pressure (i.e. the desired x_{CO2}) and waited until the contents reached equilibrium before spectral acquisition. Multiple cell loadings with different initial liquid volumes were used in order to present the entire solvent composition range, and the data show a consistent trend. The scattering of the data in Figure 3.4 indicates the uncertainty of these measurements, which is fairly satisfactory.

Kosower's *Z*-value for a given solvent is obtained by Equation 3-3, where λ (in nm) is the wavelength of maximum absorbance of 1-ethyl-4-carbomethoxypyridinium:

$$Z = \frac{2.859 \times 10^4}{\lambda} \qquad \text{Equation 3-3}$$

Results and Discussion

Solvatochromic probes

Our results for the Kamlet-Taft π^* in CO_2-expanded acetonitrile, shown in Figure 3.4, were previously reported in Chapter II as well as in the literature.[19] The key feature of the curve is that the π^* value decreases gradually with increasing CO_2 concentration below $x_{CO2} = 0.85$, then drops dramatically toward the value found for pure CO_2. The shape of the curve suggests preferential solvation of the probe by acetonitrile, as is often observed with mixed solvents.[26-28] This figure also illustrates the ability to tune the polarity of GXLs over a wide range: acetonitrile ($\pi^* = 0.75$) is slightly more polar than methanol ($\pi^* = 0.6$), but the resulting GXL can be tuned to a polarity as low as cyclohexane ($\pi^* = 0$).

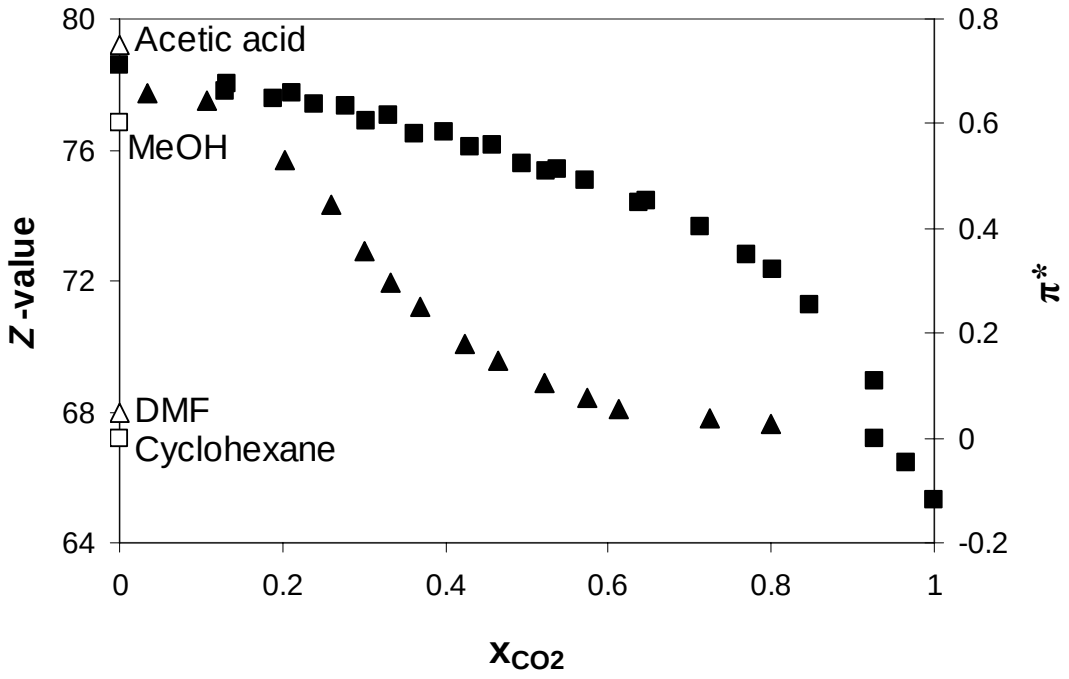

Figure 3.4. π^* and Z-value for CO_2-expanded acetonitrile as a function of composition. (□) π^* values plotted on right axis (previously reported).[19] (■) Z-values plotted on left axis. Literature values for pure solvents: (□) π^* values plotted on right axis, (Δ) Z-values plotted on left axis.[21, 29]

The Z-value of CO_2-expanded acetonitrile decreases monotonically as a function of CO_2 composition (see Figure 3.4). The addition of CO_2 continuously tunes the polarity of acetonitrile ($Z \sim 78$, cf. $Z \sim 79$ for acetic acid) in pure form to Z-values similar to *N,N*-dimethylformamide ($Z \sim 68$) at CO_2 mole fraction of ~ 0.8; the overall change in Z-value is modest. The results remain consistent with the presence of an acetonitrile-rich solvation shell within the cybotactic region surrounding the probe molecule. However, due to insolubility of the probe molecule at high CO_2 loadings, we were able to measure Z-values only for $x_{CO2} < 0.80$.

Menschutkin reaction

Figure 3.5 shows the kinetic results for the S_N2 reaction of TBA and MNBS in CO_2-expanded acetonitrile at 40ºC. The trend in the rate constants is remarkably similar to that of π^*, with a gradual decrease at low CO_2 loadings followed by a sharper descent at higher CO_2 compositions. As with the solvatochromic measurements, these data suggest preferential solvation of the probe (in this case, the reactants) by acetonitrile. Attempts to gather kinetic data at $x_{CO2} > 0.90$ failed due to limited solubility of the reactants in the CO_2-rich GXL.

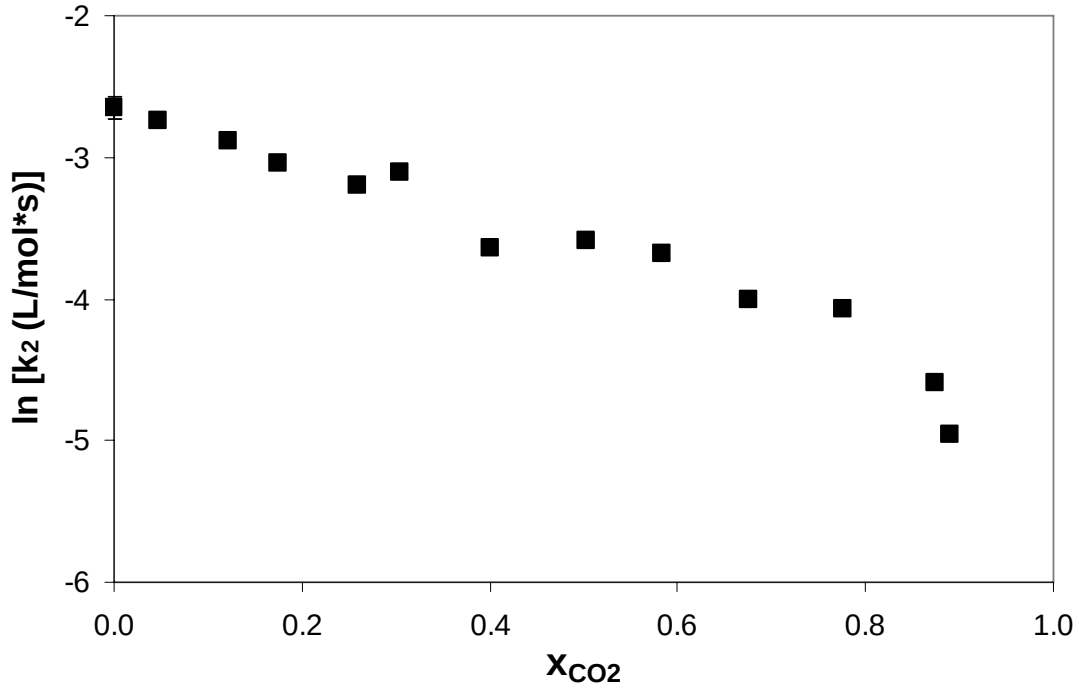

Figure 3.5: S_N2 rate constant for CO_2-expanded acetonitrile at 40ºC as a function of composition.

Local Composition Enhancement

To further understand the kinetic and solvatochromic behavior observed in CO_2-expanded acetonitrile, we investigated the local composition enhancement of acetonitrile around the probes used in the GXL. We calculated the local mole fraction of acetonitrile

($x_{ACN,local}$) based on our π^* measurements using procedures detailed in the literature.[16, 17, 31, 44, 45] To determine $x_{ACN,local}$, we first calculated the deviation in π^* ($\Delta\pi^*$) from a mole-fraction-weighted "bulk" prediction based on the values in pure acetonitrile (π^*_{ACN}) and pure CO_2 (π^*_{CO2}) over the entire solvent composition range:[31]

$$\Delta\pi^* = \pi^* - (x_{ACN,bulk}\pi^*_{ACN} + x_{CO2,bulk}\pi^*_{CO2}) \qquad \text{Equation 3-4}$$

We then assume that $\Delta\pi^* = 0$ and the bulk concentrations of the acetonitrile and CO_2 sum to 1 in order to calculate $x_{ACN,local}$.

In Figure 3.6, we plot $x_{ACN,local}$ and $x_{ACN,bulk}$ (bulk acetonitrile mole fraction) as functions of the bulk CO_2 mole fraction ($x_{CO2,bulk}$). Since $x_{ACN,local}$ was calculated based on π^*, we observe similar trends for these values. Our results for $x_{ACN,local}$ in CO_2-expanded acetonitrile are similar to those reported by Striolo et al. using a phenol blue spectroscopic probe.[18] We then define the composition enhancement factor (CEF) as:

$$CEF = \frac{x_{ACN,local}}{x_{ACN,bulk}} \qquad \text{Equation 3-5}$$

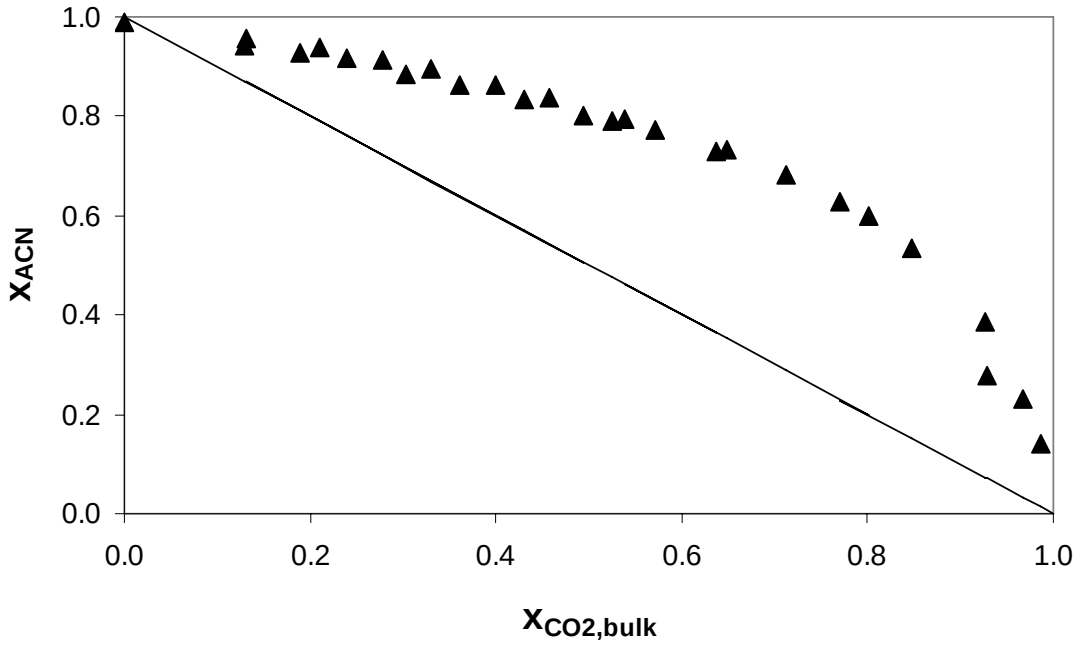

Figure 3.6: Local (▲) and bulk (—) mole fractions of acetonitrile in CO_2-expanded acetonitrile.

A plot of CEF versus x_{CO2} is shown in Figure 3.7. This curve shows only a modest change for $x_{CO2} < 0.60$ with CEF ≤ 2. At higher CO_2 loadings, the CEF increases noticeably to CEF > 10. The point of the transition between these two regions of the curve was chosen somewhat arbitrarily as $x_{CO2} = 0.60$ based on the transition from a fairly linear region of the curve to a region of the curve where the slope changes more dramatically, but the transition clearly occurs in the range $0.50 < x_{CO2} < 0.70$. The choice of a different transition point within this range would have a limited effect on the results of our subsequent analyses.

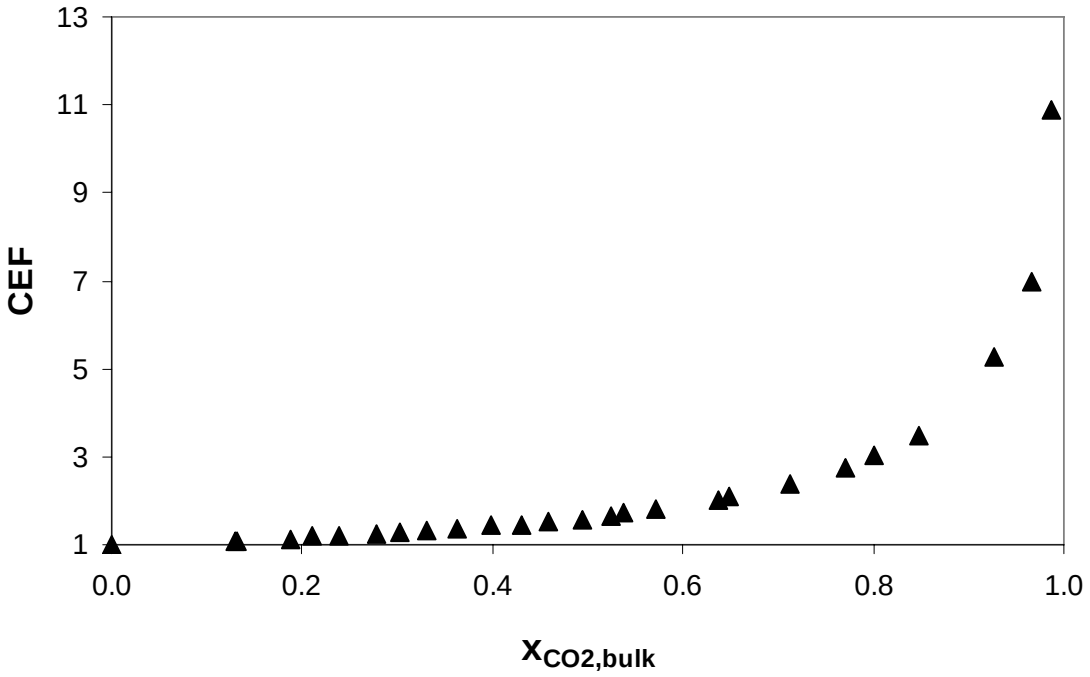

Figure 3.7: Composition enhancement factor for CO_2-expanded acetonitrile.

With this transition point in mind, we have plotted the rate of our S_N2 reaction of TBA and MNBS versus π^* for CO_2-expanded acetonitrile in Figure 3.8. If we divide the kinetic data on either side of the transition point and linearly correlate the data at $x_{CO2} < 0.60$, we see that the points for $x_{CO2} > 0.60$ diverge from the linear regression.

To further illustrate the solvation effects on the kinetics due to the local composition heterogeneity, we calculated a predicted $ln\ k_2$ value based on the linear regression in Figure 3.8. In Figure 3.9, we show the experimental kinetic data and the curve for the predicted $ln\ k_2$, both as functions of x_{CO2}. Here we see that at $x_{CO2} > 0.60$, the value of the rate constant is significantly higher than what we would predict based on our kinetic and solvatochromic data for $x_{CO2} < 0.60$.

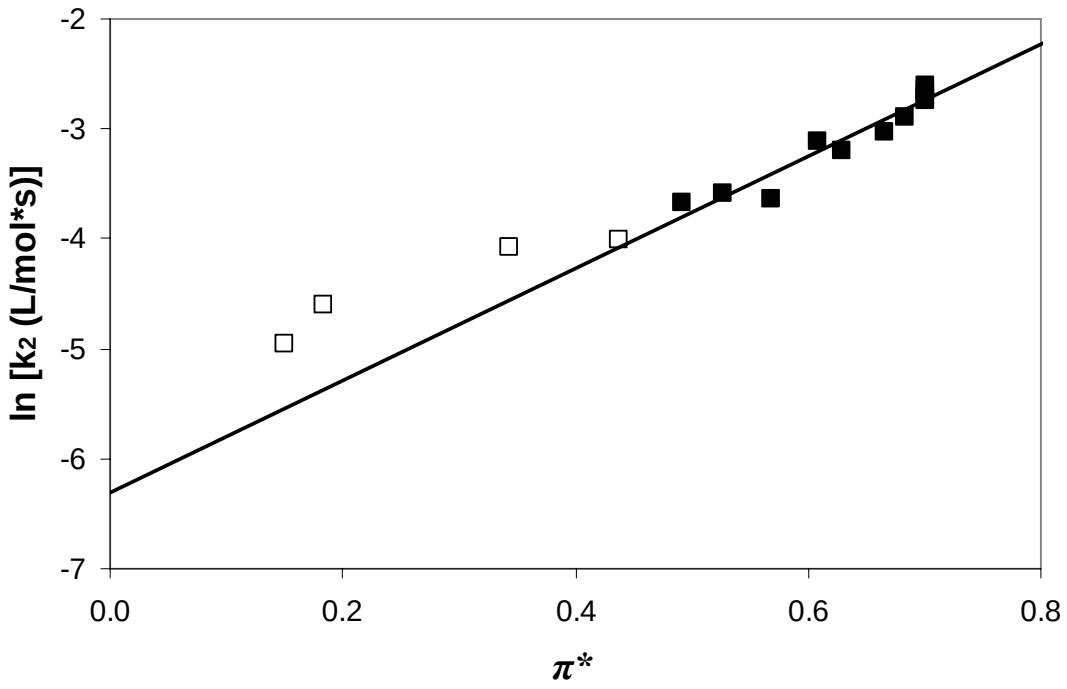

Figure 3.8: S_N2 rate constant versus π^* for CO_2-expanded acetonitrile at 40°C. Trendline (–) is the linear regression of the data based on $x_{CO2} < 0.60$. (■) Kinetic data for $x_{CO2} < 0.60$ included in the linear regression. (□) Kinetic data for $x_{CO2} > 0.60$.

Several possible causes may contribute to the observed rate enhancement at higher CO_2 loadings. Transition state stabilization by acetonitrile is one potential source of this enhancement. Since the charge-separated transition state should be stabilized in acetonitrile relative to CO_2, and we observe much more dramatic composition enhancement of acetonitrile at high CO_2 loadings than we would predict based on lower CO_2 loadings (e.g. Figure 3.7), this hypothesis seems to be supported by the data.

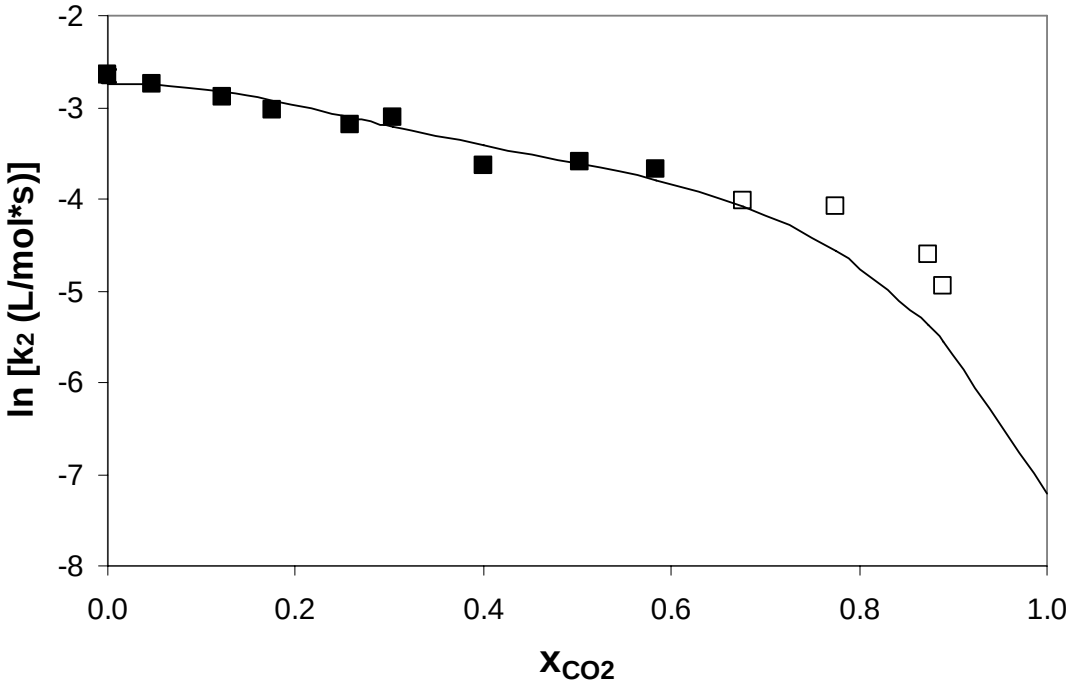

Figure 3.9: Experimental and predicted values of the S_N2 rate constant for CO_2-expanded acetonitrile at 40ºC as a function of composition. (■) Kinetic data for $x_{CO2} < 0.60$. (□) Kinetic data for $x_{CO2} > 0.60$. (–) Trendline for *ln* k_2 vs. π^* data from Figure 8, on mole fraction basis.

Another source of this deviation from bulk behavior could be clustering and/or aggregation of polar solutes (i.e. reactants) in the increasingly nonpolar GXL. Experimental evidence of enhanced kinetics by solute-solute clustering has been previously reported in literature.[46] This aggregation can lead to an increased number of collisions of the reacting species, accelerating the reaction beyond what would be expected based on bulk compositions.

Conclusions

We have examined the kinetics of a nucleophilic reaction as well as solvatochromic probes to gain insights into local solvent polarity in CO_2-expanded

acetonitrile as a function of CO_2 composition. We calculated the local composition enhanced factor and correlated the rate constants based on the solvatochromic parameters. Both the kinetic and solvatochromic behaviors support our hypothesis of the enhanced local solvent structure in the cybotactic region: Polar molecules such as acetonitrile tend to associate with the solvatochromic probes and the reactants to enhance their local compositions in the GXL. In addition to the solute-solvent clustering, we have also demonstrated the possible occurrence of enhanced solute-solute interaction at high the CO_2 composition range. These local composition enhancement phenomena can have a significant impact on reactions, as observed in this work, as well as separations such as gas-antisolvent crystallization.

While this work has focused on local composition in CO_2-expanded acetonitrile, other GXLs may prove interesting as well. A similar study with another polar aprotic solvent such as tetrahydrofuran, or a different expansion gas such as ethane, may help to determine the role of specific molecular interactions on the behavior observed in this study.

References

1. Jessop, P. G.; Subramaniam, B., Gas-expanded liquids. *Chem. Rev.* **2007,** *107*, 2666.

2. Anand, M.; McLeod, M. C.; Bell, P. W.; Roberts, C. B., Tunable solvation effects on the size-selective fractionation of metal nanoparticles in CO_2 gas-expanded solvents. *J. Phys. Chem. B* **2005,** *109*, 22852.

3. Jung, J.; Perrut, M., Particle design using supercritical fluids: literature and patent survey. *J. Supercritical Fluids* **2001,** *20*, 179.

4. Sencar-Bozic, P.; Srcic, S.; Knez, Z.; Kerc, J., Improvement of nifedipine dissolution characteristics using supercritical CO_2. *Int. J. Pharm.* **1997,** *148*, 123.

5. Johnson, C. A.; Sharma, S.; Subramaniam, B.; Borovik, A. S., Nanoparticulate metal complexes prepared with compressed carbon dioxide: correlation of particle morphology with precursor structure. *J. Am. Chem. Soc.* **2005,** *127*, 9698.

6. M. Chandler McLeod, M. A., Christopher L. Kitchens, and; Roberts*, C. B., Precise and rapid size selection and targeted deposition of nanoparticle populations using CO_2 gas expanded liquids. *Nano Lett.* **2005,** *5* (3), 461.

7. McLeod, M. C.; Kitchens, C. L.; Roberts, C. B., CO_2-expanded liquid deposition of ligand-stabilized nanoparticles as uniform, wide-area nanoparticle films. *Langmuir* **2005,** *21*, 2414.

8. Song, I.; Spuller, M.; Levitin, G.; Hess, D. W., Photoresist and residue removal using gas-expanded liquids. *J. Electrochem. Soc.* **2006,** *153* (4), G314.

9. Jin, H.; Subramaniam, B., Homogeneous catalytic hydroformylation of 1-octene in CO_2-expanded solvent media. *Chem. Eng. Sci.* **2004,** *59*, 4887.

10. Jin, H.; Subramaniam, B.; Ghosh, A.; Tunge, J., Intensification of catalytic olefin hydroformylation in CO_2-expanded media. *AIChE J.* **2006,** *52* (7), 2575.

11. Kerler, B.; Robinson, R. E.; Borovik, A. S.; Subramaniam, B., Application of CO_2-expanded solvents in heterogeneous catalysis: a case study. *Appl. Cat. B: Env.* **2004,** *49*, 91.

12. Hill, E. M.; Broering, J. M.; Hallett, J. P.; Bommarius, A. S.; Liotta, C. L.; Eckert, C. A., Coupling chiral homogeneous biocatalytic reactions with benign heterogeneous separation. *Green Chem.* **2007,** *9*, 888.

13. Lu, J.; Lazzaroni, M. J.; Hallett, J. P.; Bommarius, A. S.; Liotta, C. L.; Eckert, C. A., Tunable solvents for homogeneous catalyst recycle. *Ind. Eng. Chem. Res.* **2004,** *43*, 1586.

14. Jones, R. S. Carbon dioxide as a benign solvent for homogeneous catalyst recovery and recycle. Ph.D. Thesis, Georgia Institute of Technology, Atlanta, GA, 2005.

15. Gurdial, G. S.; Macnaughton, S. J.; Tomasko, D. L.; Foster, N. R., Influence of chemical modifiers on the solubility of *o*- and *m*-hydroxybenzoic acid in supercritical CO_2. *Ind. Eng. Chem. Res.* **1993,** *32*, 1488.

16. Kim, S.; Johnston, K. P., Clustering in supercritical fluid mixtures. *AIChE J.* **1987,** *33* (10), 1603.

17. Roberts, C. B.; Brennecke, J. F.; Chateauneuf, J. E., Solvation effects on reactions of triplet benzophenone in supercritical fluids. *AIChE J.* **1995,** *41* (5), 1306.

18. Striolo, A.; Elvassore, N.; Parton, T.; Bertucco, A., Relationship between volume expansion, solvent power, and precipitation in GAS processes. *AIChE J.* **2003,** *49* (10), 2671.

19. Ford, J. W.; Lu, J.; Liotta, C. L.; Eckert, C. A., Solvent effects on the kinetics of a Diels-Alder reaction in gas-expanded liquids. *Ind. Eng. Chem. Res.* **2007**, In press.

20. Reichardt, C., Solvatochromic dyes as solvent polarity indicators. *Chem. Rev.* **1994,** *94*, 2319.

21. Marcus, Y., The properties of organic liquids that are relevant to their use as solvating solvents. *Chem. Soc. Rev.* **1993**, 409.

22. Kamlet, M. J.; Abboud, J.-L. M.; Taft, R. W., The solvatochromic comparison method. 6. The π* scale of solvent polarities. *J. Am. Chem. Soc.* **1977,** *99* (18), 6027.

23. Nicolet, P.; Laurence, C., Polarity and basicity of solvents. Part 1. A thermosolvatochromic comparison method. *J. Chem. Soc., Perkin Trans. II* **1986**, 1071.

24. Laurence, C.; Nicolet, P.; Helbert, M., Polarity and basicity of solvents Part 2. Solvatochromic hydrogen-bonding shifts as basicity parameters. *J. Chem. Soc., Perkin Trans. II* **1986**, 1081.

25. Lu, J.; Brown, J. S.; Boughner, E. C.; Liotta, C. L.; Eckert, C. A., Solvatochromic characterization of near-critical water as a benign reaction medium. *Ind. Eng. Chem. Res.* **2002,** *41*, 2835.

26. Mellein, B. R.; Aki, S. N. V. K.; Ladewski, R. L.; Brennecke, J. F., Solvatochromic studies of ionic liquid/organic mixtures. *J. Phys. Chem. B* **2007,** *111* 131.

27. Fredlake, C. P.; Muldoon, M. J.; Aki, S. N. V. K.; Welton, T.; Brennecke, J. F., Solvent strength of ionic liquid/CO_2 mixtures. *Phys. Chem. Chem. Phys.* **2004,** *6*, 3280.

28. Wyatt, V. T.; Bush, D.; Lu, J.; Hallett, J. P.; Liotta, C. L.; Eckert, C. A., Determination of solvatochromic solvent parameters for the characterization of gas-expanded liquids. *J. Supercritical Fluids* **2005,** *36*, 16.

29. Kosower, E. M., The effect of solvent on spectra. I. A new empirical measure of solvent polarity: *Z*-values. *J. Am. Chem. Soc.* **1958,** *80*, 3253.

30. Lu, J.; Liotta, C. L.; Eckert, C. A., Spectroscopically probing microscopic solvent properties of room-temperature ionic liquids with the addition of carbon dioxide. *J. Phys. Chem. A* **2003,** *107*, 3995.

31. Yonker, C. R.; Smith, R. D., Solvatochromic behavior of binary supercritical fluids: the carbon dioxide/2-propanol system. *J. Phys. Chem.* **1988,** *92*, 2374.

32. Sigman, M. E.; Lindley, S. M.; Leffler, J. E., Supercritical carbon dioxide: Behavior of π* and β solvatochromic indicators in media of different densities. *J. Am. Chem. Soc.* **1985,** *107*, 1471.

33. Mancini, P. M.; Fortunato, G.; Adam, C.; Vottero, L. R.; Terenzani, A. J., Specific and non-specific solvent effects on aromatic nucleophilic substitution. Kinetics of the reaction of 1-fluoro-2,6-dinitrobenzene and homopiperidine in binary solvent mixtures. *J. Phys. Org. Chem.* **2002,** *15*, 258.

34. Migron, Y.; Marcus, Y., Polarity and hydrogen-bonding ability of some binary aqueous-organic mixtures. *J. Chem. Soc. Faraday Trans.* **1991,** *87* (9), 1339.

35. Kosower, E. M., *An Introduction to Physical Organic Chemistry*. John Wiley & Sons, Inc.: New York, 1968.

36. Reichardt, C., *Solvents and Solvent Effects in Organic Chemistry*. 2nd ed.; John Wiley and Sons: New York, 1988.

37. Lowry, T. H.; Richardson, K. S., *Mechanism and Theory in Organic Chemistry*. 3rd ed.; Harper Collins: New York, 1987.

38. Abboud, J. L. M.; Notario, R.; Bertran, J.; Sola, M., One Century of Physical Organic Chemistry: The Menschutkin Reaction. In *Progress in Physical Organic Chemistry*, Taft, R. W., Ed. John Wiley and Sons: New York, 1993; Vol. 19.

39. Skrzypczak, A.; Neta, P., Rate constants for reaction of 1,2-dimethylimidazole with benzyl bromide in ionic liquids and organic solvents. *Int. J. Chem. Kinetics* **2004,** *36* (4), 253.

40. Crowhurst, L.; Lancaster, N. L.; Arlandis, J. M. P.; Welton, T., Manipulating solute nucleophilicity with room temperature ionic liquids. *J. Am. Chem. Soc.* **2004,** *126*, 11549.

41. Sola, M.; Lledos, A.; Duran, M.; Bertran, J.; Abboud, J. L. M., Analysis of solvent effects on the Menshutkin reaction. *J. Am. Chem. Soc.* **1991,** *113* (8), 2873.

42. Lazzaroni, M. J.; Bush, D.; Brown, J. S.; Eckert, C. A., High-pressure vapor-liquid equilbria of some carbon dioxide + organic binary systems. *J. Chem. Eng. Data* **2005,** *50*, 60.

43. Lancaster, N. L.; Welton, T.; Young, G. B., A study of halide nucleophilicity in ionic liquids. *J. Chem. Soc., Perkin Trans. II* **2001**, 2267.

44. Zhang, J.; Lee, L. L.; Brennecke, J. F., Fluorescence spectroscopy and integral equation studies of preferential solvation in supercritical fluid mixtures. *J. Phys. Chem.* **1995,** *99*, 9268.

45. Zhang, J.; Roek, D. P.; Chateauneuf, J. E.; Brennecke, J. F., A steady-state and time-resolved fluorescence study of quenching reactions of anthracene and 1,2-benzanthracene by carbon tetrabromide and bromoethane in supercritical carbon dioxide. *J. Am. Chem. Soc.* **1997,** *119*, 9980.

46. Kajimoto, O., Solvation in supercritical fluids: its effects on energy transfer and chemical reactions. *Chem. Rev.* **1999,** *99* (355-389).

CHAPTER IV

ORGANIC-AQUEOUS TUNABLE SOLVENTS FOR 1-OCTENE HYDROFORMYLATION AND CATALYST RECYCLE

Introduction

Aqueous biphasic catalysis is used industrially to sequester a catalyst for easy catalyst recycle, where a water-soluble catalyst is deployed in an aqueous phase, while the reactant is in an organic phase.[1-3] This approach is used industrially for the hydroformylation of ethylene and propylene,[4,5] but even for these processes intense mixing is required to overcome the mass-transfer limitations imposed by the low solubility of organic substrates in the (catalyst-containing) aqueous phase. The process is not useful for olefins with more than four carbon atoms as the water solubility is far too low, leading to severe mass transfer limitations on the reaction.[6] Here we report a new method for performing such reactions homogeneously, and show as an example the successful hydroformylation of an eight carbon olefin, 1-octene (see Figure 4.1). Clearly this method could be applied for many other reactions.

Gas-expanded liquids (GXLs), generally mixtures of organic solvents with some gas, most often CO_2, at moderate pressures (3 to 8 MPa), are benign, highly-tunable solvents offering advantages for separations, reactions, and advanced materials.[7-9] GXLs are intermediate in properties between normal liquids and supercritical fluids, both in solvating power and in transport properties, and these properties are highly tunable by simple pressure variations. GXLs have been used for a variety of applications, including gas-antisolvent (GAS) crystallization,[10,11] particle production,[12] and as a reaction solvent.[13-18]

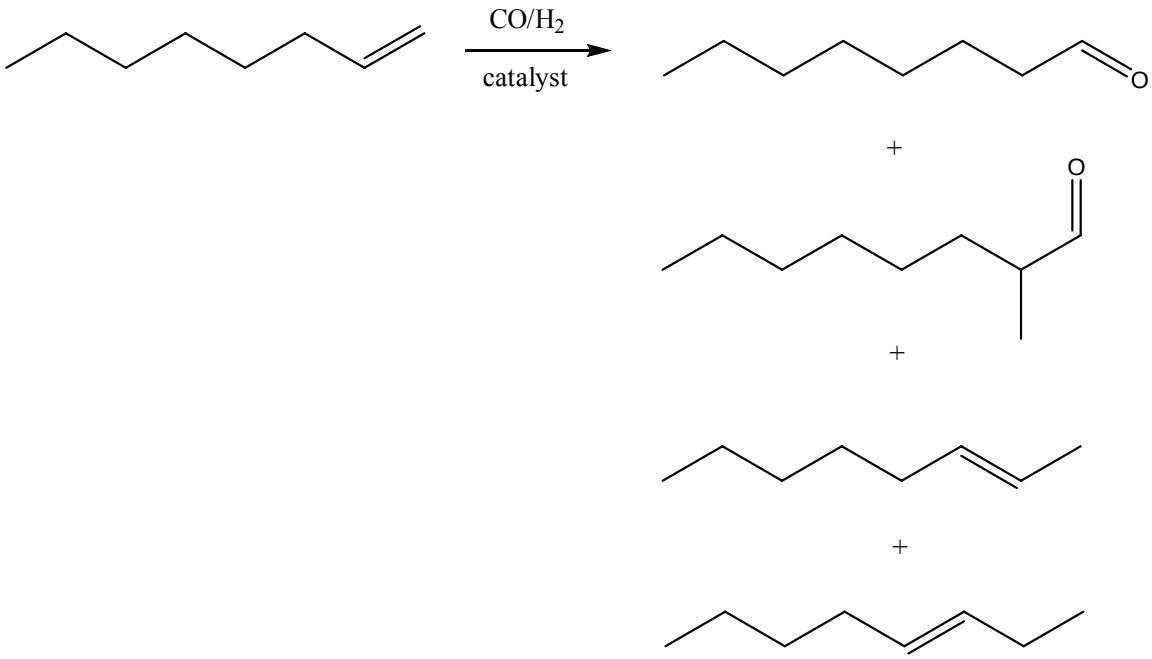

Figure 4.1: Hydroformylation of 1-octene. Linear and branched aldehyde products and isomerization side products are shown.

We have used **O**rganic-**A**queous **T**unable **S**olvents (**OATS**),[19-21] with gaseous CO_2 as an antisolvent to separate a miscible mixture into an aqueous phase and a gas-expanded organic phase. Although little CO_2 dissolves in water, it is quite miscible with most organics, and radically lowers the solvent power of the organic phase for ions and other polar compounds.[22] This permits ready dissolution of hydrophobic substrates in the organic-aqueous mixture for reaction, and facile separation of hydrophobic products and unreacted substrate with the gas-expanded liquid after CO_2 addition. The use of a hydrophilic catalyst permits facile recycle with the aqueous phase. Additionally, we can control the quality of the phase split and the partition values by adjusting the CO_2 pressure. Finally, after decantation of the gas-expanded organic phase, depressurization permits CO_2 recycle and simplified product purification. The organic cosolvent also

enhances the desirable solubility of higher olefins for reactions; note for example that propylene is soluble in water at 200 ppm (by mass) while 1-octene is soluble at only 2.7 ppm.[23] The 1-octene solubility limit can be overcome by the addition of tetrahydrofuran (THF) co-solvent; in a 70% (v/v) THF/water mixture the solubility increases more than 10,000-fold.[24]

Other researchers have explored methods to increase the reaction rates of higher order olefins in aqueous biphasic systems. One approach was the addition of cosolvents,[25] but the cosolvent hindered the separation process.[26] The use of a traditional cosolvent system suffered from the non-ligated catalyst leaching into the organic phase. This unacceptable catalyst leaching and product poisoning is not experienced in the traditional Ruhrchemie/Rhone-Poulenc process.[27]

Another method involves using surface active ligands rather than the traditional TPPTS (triphenylphosphine trisulfonate sodium salt).[28] These surface active ligands do show increased yields for the hydroformylation of 1-octene; however the yields drop off again as the size of the substrate is increased. That work does not include any discussion of catalyst leaching, which is a potential problem when employing surface active species, as the surface active ligands will also have a measurable solubility in the organic phase, again hindering the separation of the catalyst from the desired products.

Experimental

Materials

THF and water used in the experiments were HPLC grade, obtained from Sigma-Aldrich Chemical Company. The HPLC water and THF were degassed using the freeze-pump-thaw method on a Schlenk line apparatus. SFC Grade carbon dioxide (99.99%)

was obtained from Air Gas. The CO_2 was further purified to remove trace water using a Matheson (Model 450B) gas purifier and filter cartridge (Type 451). UHP grade syngas (1:1 $CO:H_2$) was obtained from AirGas and used as received. 1-octene (98%), nonan-1-al (≥95%), the catalyst (Acetylacetonato)dicarbonylrhodium(I) (98%), as well as the triphenylphosphine (99%), triphenylphosphine monosulfonate (TPPMS) sodium salt (≥90%), and TPPTS (≥95%) ligands were purchased from Sigma-Aldrich Chemical Company and used as received.

Apparatus and Procedure

Hydroformylation reactions were carried out in a 300 mL stainless steel autoclave reactor (Parr Instrument Company, Model 4561) with a maximum working pressure of 208 bar and a maximum working temperature of 350°C. A magnetic stir-drive (Parr Instrument Company, Model A1120HC) equipped with a four-blade 85° pitched-blade impeller provided stirring. A PTFE gasket constituted the seal between the stirrer and the reactor, and a flat PTFE gasket held in a confined recess in the reactor head sealed the reactor head to the reactor body. The internal volume of the reactor was 305 mL, based on multiple loadings of a known mass of pure CO_2 and pressure measurements at several temperatures.

A PID temperature controller and tachometer (Parr Instrument Company, Model 4842) were used to control the temperature of the reactor to ± 1°C and the stirring speed to ± 5 rpm. The temperature inside the reactor was monitored with a type J thermocouple and heat was provided by a high-temperature heating mantle housed in an aluminum shell. A digital pressure transducer (Heise, Model 901B) was used to monitor constantly

the reactor pressure, and a safety rupture disk, made of Inconel, was used to ensure the pressure in the reactor remained below the reactor pressure rating.

We modified the Parr reactor by replacing all of the standard valves and fittings with low volume HiP valves and fittings to decrease the reactor dead volume. After evacuating the reactor to vacuum for 20 minutes, we loaded syngas through stainless steel tubing (3.18 mm OD and 1.52 mm ID) to a second inlet port. We then flushed the reactor three times with approximately 3.5 bar syngas (STP) before adding catalyst precursor and ligand solutions using Hamilton SampleLock gas-tight syringes with luer locks. Next we added 15 mL degassed water and 35 mL degassed THF using gas-tight syringes.

After loading solutions of the rhodium catalyst and the desired ligand, the reactor was heated to the desired temperature while the catalyst was formed *in situ* under mild syngas pressure. Next we introduced 1 mL of 1-octene with a syringe and pressurized the reactor to approximately 31 bar with syngas to start the reaction. The initial concentrations of the rhodium catalyst, the ligand, and 1-octene were 2.5×10^{-7} mol/L, 2.5×10^{-6} mol/L, and 1.27×10^{-4} mol/L, respectively. These concentrations represent a 10:1 molar ratio of ligand to catalyst and a 500:1 molar ratio of substrate to catalyst. After reaction, typically about one hour, we quenched the reactor with an ice bath, and then depressurized through stainless steel tubing submerged in THF to catch any volatiles. The reactor contents were added to the THF and analyzed using an Agilent GC-FID (model 6890). External standards of known concentration of 1-octene and nonan-1-al were used to calibrate the FID response.

Catalyst Synthesis

For a limited number of experiments, the catalyst was synthesized prior to the reaction using a method set forth by Ahmad.[29] The synthesis was performed under a N_2 atmosphere since the desired phosphine ligands were water-soluble and air sensitive. All solvents used in the synthesis were degassed prior to use using three freeze-pump-thaw cycles on a Schlenk line apparatus. The synthesis and purification were also done on the Schlenk line. The catalyst synthesis was performed in a mixture of water and ethanol to ensure the solubility of both the phosphine and the catalyst precursor.

Recycle Experiments

To demonstrate catalyst recovery without loss of activity, we performed a series of experiments to reuse the catalyst after the phase separation. We used a windowed version of the Parr vessel, fitted with a dip tube to draw out the organic phase under pressure. We used the same method, with bookkeeping for water filled and drawn off to determine the volume below the dip tube. A high pressure syringe pump (ISCO, Inc., Model 500D) supplied CO_2 for phase separation and maintained constant pressure during removal of the organic phase, via one inlet port on the reactor head. Using this technique, the organic product phase could be removed for analysis and a fresh reactant mixture added for each cycle.

Results and Discussion

Ligand Partitioning

The partitioning of the catalyst complex in the CO_2-induced biphasic system represents a key variable in the design of an industrial process, as easy catalyst recovery is the biggest advantage of a biphasic system over a monophasic one. Partition coefficient measurements on the TPPTS (triphenylphosphine trisulfonate sodium salt)

and TPPMS (triphenylphosphine monosulfonate sodium salt) ligands (Figure 4.2) were performed in a high pressure UV-vis cell.[30] In the absence of CO_2, both ligands were completely soluble in the mixed solvent. The partitioning of the ligand was then measured as a function of added CO_2 pressure for the CO_2-induced biphasic system. The partition coefficients are reported as the ratio of the ligand concentration in the aqueous phase to the ligand concentration in the organic phase, as determined by the UV measurements. For the TPPTS ligand, the partition coefficient in a 70:30 (v:v) THF:H_2O mixture varied from 1400 to 4100 as the CO_2 pressure was increased from 20 bar to 50 bar (Figure 4.3). The partition coefficients for TPPMS were slightly lower, varying from 1000 to 2600 from 17 bar to 44 bar. This result is expected, as the addition of more salt groups would make the ligand more hydrophilic, increasing the partitioning into the aqueous phase. Partitioning of non-sulfonated TPP failed — the ligand was insoluble in the aqueous phase.

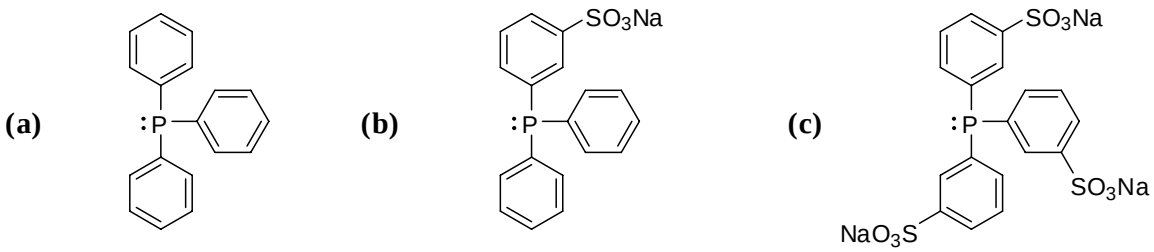

Figure 4.2: Catalyst ligands (a) Triphenylphosphine (TPP) (b) Triphenylphosphine mono-sulfonated sodium salt (TPPMS) (c) Triphenylphosphine tris-sulfonated sodium salt (TPPTS).

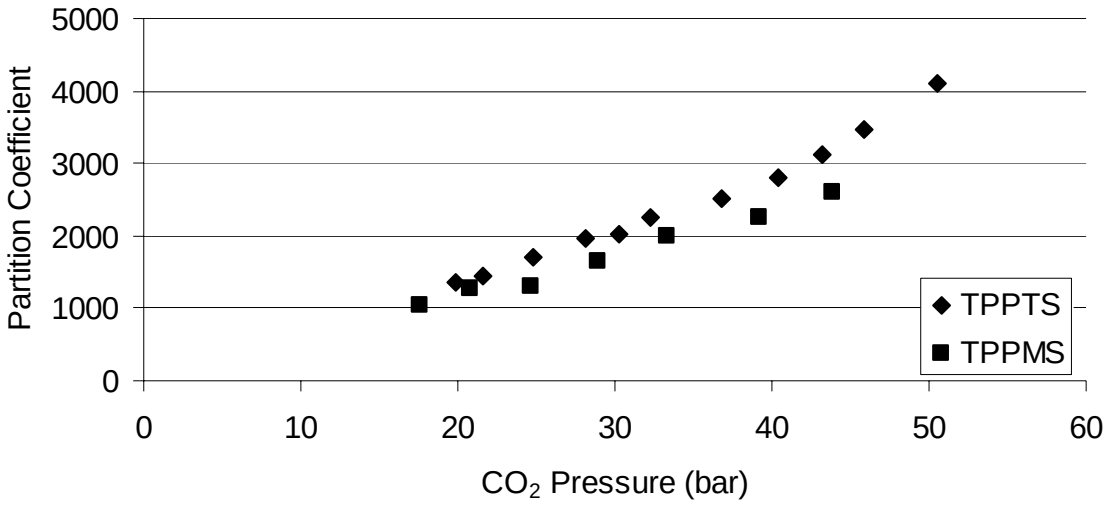

Figure 4.3: Partition coefficient of TPPTS and TPPMS ligands in 70:30 (v:v) mixture of THF/water as a function of CO_2 pressure.

The measured partition coefficients for both TPPMS and TPPTS would ensure catalyst recoveries >99.9% at all measured pressures. It is also noteworthy that these partition coefficients are comparable to those for both aqueous biphasic[2,3] and fluorous biphasic[31] schemes reported in the literature. Maintaining excellent partitioning coefficients is a key factor in the economic efficiency of any biphasic catalytic reaction, as both the metal and ligand costs are often significant. Our ability to maintain catalyst recovery while using the commercially available water-soluble ligands (rather than specialty ligands) will also help keep overall processing costs down. Because the pressures ranges employed for this recycle (15-50 bar) are similar to the actual reaction (31 bar) the use of specialized high pressure equipment for the separation will not add to the overall cost of a potential process, as it often does for supercritical extractions.[32] Also the catalyst complex may partition at a different rate than the uncomplexed ligands; in our recycling experiments this difference could only be measured via rhodium leaching.

Product Partitioning

The easy recovery of the products (nonanals) from the CO_2-induced biphasic system provides an added boost to the efficiency of the overall process by simplifying the downstream product purification. The dilute partitioning of 1-octene and nonan-1-al between the water rich and organic rich phase was measured as a function of added carbon dioxide in the carbon dioxide + tetrahydrofuran + water ternary system (Figure 4.4). The 1-octene partitioning results have been previously reported by our group.[22] At low pressures (7 bar) the concentration of 1-octene is 10 times greater in the tetrahydrofuran-rich phase than in the water-rich phase and increases to 3000 times greater at a pressure of just 17 bar! The nonanal partitioning was similarly high, with the partitioning varying from 8:1 at low pressure up to 2500:1 at 26 bar. The addition of small amounts of carbon dioxide was reported to cause a large change in water content in the two equilibrium phases, which greatly affects partitioning. These partition coefficients are of the same magnitude as those reported for the *n*-hexane/water/THF system (3000-23000).[24] These data establish that the recovery of the hydrophobic products and unreacted olefin from the reaction mixture will be greatly simplified by the CO_2 addition. The CO_2 pressure required for 99% recovery of nonanal (7 bar) was also much lower than the syngas pressure during the reaction (31 bar). These modest pressure requirements demonstrate the feasibility of this technique for industrial separations involving hydrophobic product recovery. Because these excellent product partition coefficients should extend to most any nonionic organic product, the use of the OATS technique with a variety of catalytic transformations will be possible.

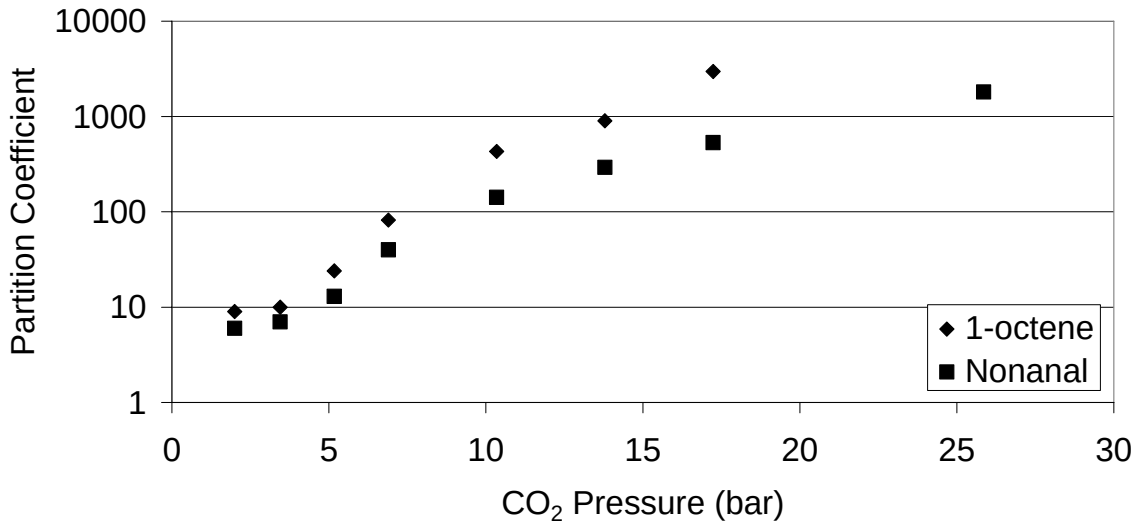

Figure 4.4: Partitioning of 1-octene and nonan-1-al between GX-THF and water as a function of CO_2 pressure. 1-octene data were previously reported.[22]

Homogeneous Catalysis

We performed the catalytic hydroformylation of 1-octene at 40°C, 80°C, and 120°C using rhodium complexes with TPPTS and TPPMS as catalyst ligands and compared these reactions to a Rh-TPP (triphenylphosphine) system in the identical mixed solvent. Reaction conditions at a given temperature, except for the choice of ligand, were identical as described above. The linear-to-branched (L/B) ratio stayed approximately constant across our temperature range at 2.1 ± 0.3 for the TPPMS system (Table 4.1). This ratio is lower than for other ligands being used for biphasic hydroformylation reactions;[2-4] but most reported results used propylene as a substrate. Since propylene cannot undergo isomerization, one path to the branched product is eliminated. Reactions utilizing TPPTS as a ligand yielded an L/B ratio of 2.3, while the L/B ratio for the TPP ligand was 2.7. The slightly higher L/B ratio for the traditional TPP ligand compared to TPPTS and TPPMS will not be a significant disadvantage for our technique provided the

ratios remain similar under different conditions or for different substrates. The stability of this ratio for a variety of OATS systems is currently under investigation.

Table 4.1: Reaction results for the monophasic (70:30 (v:v) mixture of THF/water) reactions. Each reaction was performed for one hour (except where noted) with a substrate:Rh ratio of approximately 500:1 and a ligand:metal ratio of approximately 10:1.

Ligand	T (°C)	Conversion to Aldehydes (%)	Linear to Branched Ratio	Conversion to Olefin Isomers (%)	TOF (hr^{-1})
TPPMS (synth)	120	76 ± 8	2.3 ± 0.2	19 ± 8	370 ± 50
TPPMS	120	72 ± 4	2.3 ± 0.2	20 ± 5	350 ± 20
	80	85 ± 0	2.4 ± 0.0	4 ± 0	390 ± 10
	40	21 ± 4	1.7 ± 0.2	1 ± 1	95 ± 25
TPPTS	120	38	2.86	38	115
	80	24	2.47	28	108
	40	1	1.54	1	7
TPP	120	91	2.67	0	457

The overall conversion rate of 1-octene for the three ligands in the monophasic system is fairly similar. The average overall turnover frequency, based on aldehyde yield, using TPP as the ligand was found to be 457 hr^{-1}, while for TPPTS and TPPMS we measured TOFs of 115 hr^{-1} and 350 hr^{-1}, respectively. An even larger difference between the three ligands is the product distribution or rate of isomerization side reaction. The TPPTS ligand yielded approximately equal amounts of aldehydes and olefin isomers at each temperature: 38% each of aldehydes and isomers at 120°C, 24% aldehydes and 28% isomers at 80°C and 1% each of aldehydes and isomers at 40°C (the remainder in each

case was unreacted 1-octene). Meanwhile, the TPPMS yielded 72% aldehydes and 20% olefin isomers at 120°C, 85% aldehydes and only 4% isomers at 80°C and 21% aldehydes and 1% isomers at 40°C with similar results for the *in situ* and *ex situ* (76% aldehydes and 19% isomers with a TOF = 370 hr^{-1} at 120°C) catalyst preparations. Neither sulfonated ligand system performed quite as well as the unmodified TPP system (91% aldehydes, no isomers at 120°C); however the unmodified TPP ligand complex could not be recovered using OATS. Interestingly, the TPPMS system at 80°C compares favorably with the TPP system at 120°C in terms of conversion to aldehydes (85% versus 91%, respectively) and isomers (4% versus 1%), while the TPPTS system was not competitive in either metric under any of the conditions in this study. These data suggest that the optimal conditions for these ligands differ, allowing the TPPMS system to perform better at a lower temperature than the TPP system. This finding represents a clear advantage of the OATS system in terms of catalyst activity and recyclability, and an opportunity for further optimization of the reaction conditions examined in this work.

We hypothesize that the marked difference in aldehyde:isomer ratio is caused by electronic donating effects deriving from adding the sulfonate groups in meta- position onto the phenyl rings.[33] Refer to Appendix A for additional data and discussion related to this hypothesis.

For this reason, recycle experiments were carried out using TPPMS as the ligand of choice since the salt group on the TPPMS should be enough to impart selective partitioning into the water phase while reducing the side reactions as much as possible. For comparison, we examined the biphasic reaction system consisting of 50 mL water and 1 mL 1-octene with TPPTS as the ligand. We found no isomerization after the

standard reaction time of one hour but the reaction rate was significantly lower than in the mixed water-THF solvent (see Figure 4.5). By extending the reaction time of the biphasic system to 90 hours, we were able to determine that aldehyde formation and isomerization took place in approximately the same ratios as in the monophasic system. These results were further evidence that the selectivity for aldehydes versus isomers is most likely caused by the choice of ligand.

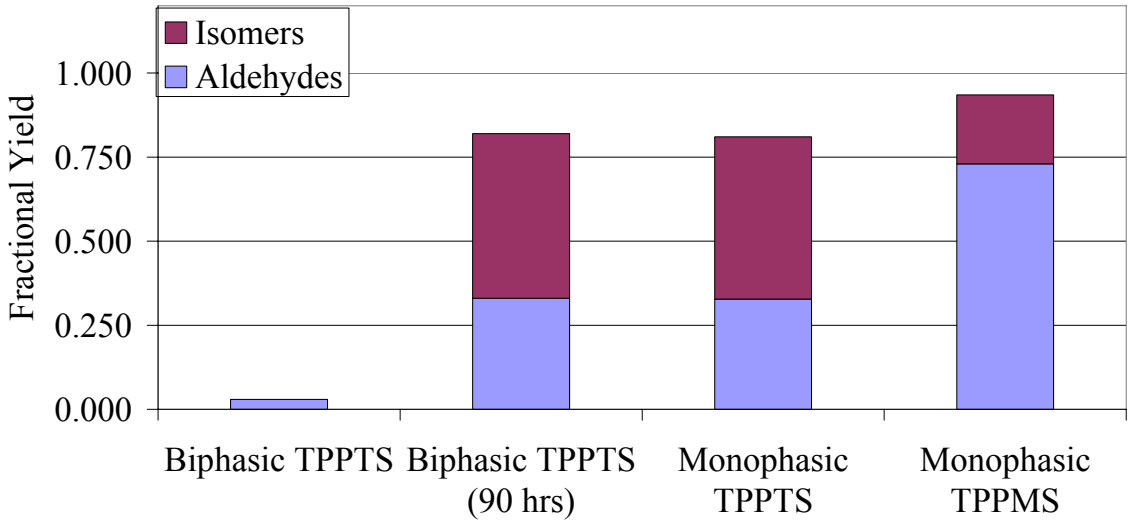

Figure 4.5: Product distributions for monophasic and biphasic hydroformylations using Rh/ligand at 120°C. Each reaction was performed for one hour (except where noted) with a substrate:Rh ratio of approximately 500:1 and a ligand:metal ratio of approximately 10:1. The monophasic systems contained a 70:30 (v:v) mixture of THF/water while the biphasic systems contained no THF.

The monophasic, or mixed solvent, system shows a marked improvement over the more common biphasic system. The turnover frequency (based on yield of aldehydes) of the biphasic system was roughly 4 hr^{-1} where the TOF (turnover frequency) for our monophasic system was 350 hr^{-1}. This is an increase of 85 fold. By changing to the TPPMS ligand we were also able to minimize the isomerization of the substrate (Figure 4.5).

Catalyst Recycle

Finally, to demonstrate that our homogeneous catalyst can be recycled, we performed the reaction three times with the organic phase being removed and refreshed after each run. The organic phase was tested with a GC-FID and calculations were based on the phase behavior of Lazzaroni *et. al.*[22] The cycles were performed at 120°C and 31 bar syngas pressure with substrate, catalyst, and ligand concentrations as stated above. Each of the separations was performed using 32 bar CO_2. The results show that the aldehyde production is approximately constant for each run (Figure 4.6) with the TOF varying from 51 hr^{-1} to 47 hr^{-1} to 54 hr^{-1} for each cycle. This constant reaction rate indicates that the recycle process does not result in any loss of activity of the catalyst and no rhodium losses were determined using AAS (detection limit <1 ppm).

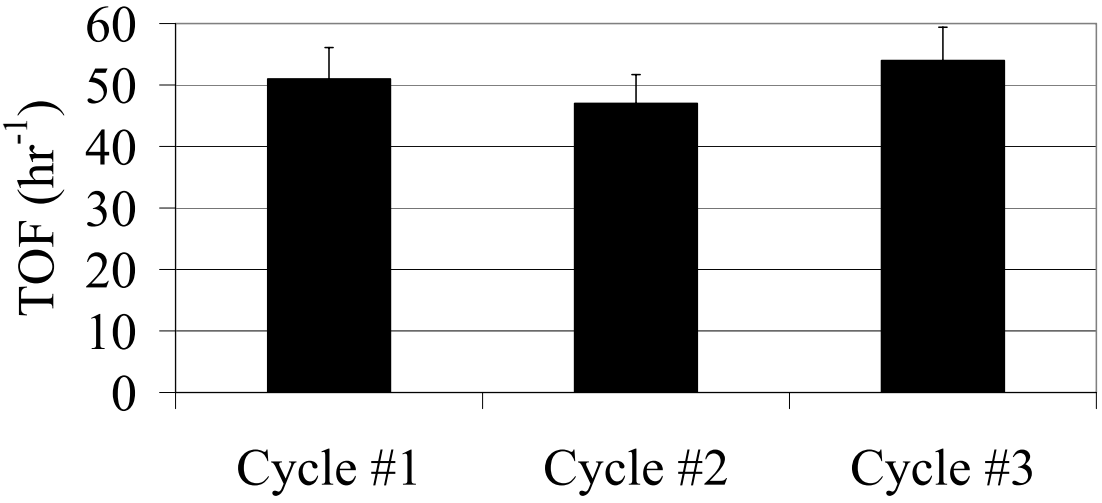

Figure 4.6: Aldehyde production (TOF) for successive hydroformylations with recycled Rh/TPPMS catalyst at 120°C. Each reaction was performed for one hour with a substrate:Rh ratio of 546:1 and a ligand:metal ratio of 10.6:1. The yield on each cycle exceeded 80%.

Conclusions

We have shown we can tailor an OATS system to improve the reaction rate of 1-octene by a factor of 85 while retaining constant reaction rate over three runs. The constant rate over three runs implies that most, if not all, of the active rhodium species was retained during separation. Full catalyst retention is also supported by the ligand partitioning data. We were also able to tailor the water soluble catalyst for the selective formation of aldehyde products from 1-octene using TPPMS as our ligand.

The addition of salt groups to the phosphine ligands does increase the olefin isomerization side-reaction. The TPPMS ligand gave relatively high selectivity to hydroformylation (approximately 21:1 at 80°C) while the TPPTS ligand yielded catalysts with approximately equal hydroformylation and isomerization activities. The ligand with two salt groups (TPPDS) is not commercially available but may be a good trade-off between water solubility and isomerization rate. It may also be possible to further insulate the charge effects by using alkyl "spacer" groups between the sulfonate moiety and the aromatic ring.[34]

Based on this demonstration of the increase in TOF by using a water-soluble catalyst in mixed solvents, with high catalyst recovery using CO_2, there should be an opportunity for hydroformylation of other, potentially more hydrophobic substrates. The composition of the aqueous-organic system can be changed in order to facilitate the dissolution of the substrate and desired water soluble catalyst.

This constitutes a strong example of the value of a tunable solvent system – we have run a homogeneous reaction with a homogeneous catalyst followed by the use of easily-removed CO_2 to effect a phase separation for product purification and facile

recycle of a hydrophilic catalyst. Clearly there exist many other opportunities to use the novel solvents.

References

1. Herrmann, W. A.; Kohlpaintner, C. W.; Manetsberger, R. B.; Bahrmann, H.; Kottmann, H. Water-soluble Metal Complexes and Catalysts. Part 7. New Efficient Water-soluble Catalysts for Two-phase Olefin Hydroformylation: BINAS-Na, a Superlative in Propene Hydroformylation. *J. Mol. Cat. A* **1995**, *97*, 65-72.

2. Horváth, I. T.; Joo, F., Eds. *Aqueous Organometallic Chemistry and Catalysis*; Kluwer: Dordrecht, 1995.

3. Cornils, B.; Herrmann, W. A., Eds. *Aqueous Phase Organometallic Catalysis - Concepts and Applications*; Wiley-VCH: Weinheim, Germany, 1998.

4. Cornils, B.; Herrmann, W. A., Eds. *Applied Homogeneous Catalysis with Organometallic Complexes*; VCH: Weinheim, Germany, 1996.

5. Cornils, B. Bulk and Fine Chemicals *via* Aqueous Biphasic Catalysis. *J. Mol. Cat. A* **1999**, *143*, 1-10.

6. Herrmann, W. A.; Kohlpaintner, C. W. Water-soluble Ligands, Metal Complexes, and Complex Catalysts: Synergism of Homogeneous and Heterogeneous Catalysis. *Angew. Chem. Int. Ed.* **1993**, *32*, 1524-1544.

7. Hallett, J. P.; Kitchens, C. L.; Hernandez, R.; Liotta, C. L.; Eckert, C. A. Probing the Cybotactic Region in Gas-Expanded Liquids (GXLs). *Acc. Chem. Res.* **2006**, *39*, 531.

8. Eckert, C. A.; Liotta, C. L.; Bush, D.; Brown, J. S.; Hallett, J. P. Sustainable Reactions in Tunable Solvents. *J. Phys. Chem. B* **2004**, *108*, 18108-18118.

9. Jessop, P. G.; Subramaniam, B. Gas-Expanded Liquids. *Chem. Rev.* **2007**, *107*, 2666-2694.

10. Winters, M. A.; Knutson, B. L.; Debenedetti, P. G.; Sparks, H. G.; Przybycien, T. M.; Stevenson, C. L.; Prestrelski, S. J. Precipitation of Proteins in Supercritical Carbon Dioxide. *J. Pharm. Sci.* **1996**, *85*, 586-594.

11. Bertucco, A.; Lora, M.; Kikic, I. Fractional Crystallization by Gas Antisolvent Technique: Theory and Experiments. *AIChE J.* **1998**, *44*, 2149-2158.

12. Bertucco, A. Precipitation and Crystallization Techniques. In *Chemical Sythnesis Using Supercritical Fluids*; Jessop, P. G., Leitner, W., Eds.; Wiley-VCH: Weinheim, 1999, p. 108-126.

13. Musie, G. T.; Wei, M.; Subramaniam, B.; Busch, D. H. Catalytic Oxidations in Carbon Dioxide-based Reaction Media, Including Novel CO_2-expanded Phases. *Coord. Chem. Rev.* **2001**, *219-221*, 789-820.

14. Wei, M.; Musie, G. T.; Busch, D. H.; Subramaniam, B. CO_2-Expanded Solvents: Unique and Versatile Media for Performing Homogeneous Catalytic Oxidations. *J. Am. Chem. Soc.* **2002**, *124*, 2513-2517.

15. West, K. N.; Culp, C. W.; McCarney, J.; Griffith, K.; Bush, D.; Liotta, C. L.; Eckert, C. A. In Situ Formation of Alkylcarbonic Acids with CO_2. *J. Phys. Chem. A* **2001**, *105*, 3947-3948.

16. Chamblee, T. S.; Weikel, R. R.; Nolen, S. A.; Liotta, C. L.; Eckert, C. A. Reversible *In Situ* Acid formation for β-pinene Hydrolysis Using CO_2 Expanded liquid and Hot Water. *Green Chem.* **2004**, *6*, 382-386.

17. Ablan, C. D.; Hallett, J. P.; West, K. N.; Jones, R. S.; Eckert, C. A.; Liotta, C. L.; Jessop, P. G. Use and Recovery of a Homogeneous Catalyst With Carbon Dioxide as a Solubility Switch. *Chem. Commun.* **2003**, 2972-2973.

18. West, K. N.; Hallett, J. P.; Jones, R. S.; Bush, D.; Liotta, C. L.; Eckert, C. A. CO_2-Induced Miscibility of Fluorous and Organic Solvents for Recycling Homogeneous Catalysts. *Ind. Eng. Chem. Res.* **2004**, *43*, 4827-4832.

19. Lu, J.; Lazzaroni, M. J.; Hallett, J. P.; Bommarius, A. S.; Liotta, C. L.; Eckert, C. A. Tunable Solvents for Homogeneous Catalyst Recycle. *Ind. Eng. Chem. Res.* **2004**, *43*, 1586-1590.

20. Broering, J. M.; Hill, E. M.; Hallett, J. P.; Liotta, C. L.; Eckert, C. A.; Bommarius, A. S. Biocatalytic Reaction and Recycling by Using CO_2-induced Organic-Aqueous Tunable Solvents. *Angew. Chem. Int. Ed.* **2006**, *45*, 4670-4673.

21. Hill, E. M.; Broering, J. M.; Hallett, J. P.; Bommarius, A. S.; Liotta, C. L.; Eckert, C. A. Coupling Chiral Homogeneous Biocatalytic Reactions with Benign Heterogeneous Separation. *Green Chem.* **2007**, 9, 888-893.

22. Lazzaroni, M. J.; Bush, D.; Jones, R.; Hallett, J. P.; Liotta, C. L.; Eckert, C. A. High-pressure Phase Equilibria of Some Carbon Dioxide-Organic-Water Systems. *Fluid Phase Equilib.* **2004**, *224*, 143-154.

23. McAuliffe, C. Solubility in Water of Paraffin, Cycloparaffin, Olefin, Acetylene, Cycloolefin, and Aromatic Hydrocarbons. *J. Phys. Chem.* **1966**, *70*, 1267-1275.

24. Robbins, G. P.; Hallett, J. P.; Bush, D.; Eckert, C. A. Liquid-liquid Equilibria and Partitioning in Organic-Aqueous Systems. *Fluid Phase Equilib.* **2007**, *253*, 48-53.

25. Monteil, F.; Queau, R.; Kalck, P. Behavior of Water-soluble Dinuclear Rhodium Complexes in the Hydroformylation Reaction of Oct-1-ene. *J. Organomet. C.* **1994**, *480*, 177-84.

26. Cornils, B. Exciting Results From the Field of Homogeneous Two-phase Catalysis. *Angew. Chem. Int. Ed.* **1995**, *34*, 1575-1577.

27. Kohlpaintner, C. W.; Fischer, R. W.; Cornils, B. Aqueous Biphasic Catalysis: Ruhrchemie/Rhone-Poulenc Oxo Process. *Appl. Cat. A* **2001**, *221*, 219-225.

28. Hanson, B. E.; Ding, H.; Kohlpaintner, C. W. Amphiphilic Phosphines for Catalysis in the Aqueous Phase. *Catal. Today* **1998**, *42*, 421-429.

29. Ahmad, N.; Robinson, S. D.; Uttley, M. F. Transition-metal Complexes Containing Phosphorus Ligands. VII. New and Improved Syntheses of Triphenylphosphine Complexes of Rhodium, Iridium, Ruthenium, and Osmium. *J. Chem. Soc., Dalton Trans.* **1972**, 843-847.

30. Dillow, A. K.; Hafner, K. P.; Yun, S. L. J.; Deng, F. H.; Kazarian, S. G.; Liotta, C. L.; Eckert, C. A. Cosolvent Tuning of Tautomeric Equilibrium in Supercritical Fluids. *AIChE J.* **1997**, *43*, 515-524.

31. Barthel-Rosa, L. P.; Gladysz, J. A. Chemistry in Fluorous Media: A User's Guide to Practical Considerations in the Application of Fluorous Catalysts and Reagents. *Coord. Chem. Rev.* **1999**, *190-192*, 587-605.

32. McHugh, M. A.; Krukonis, V. J. *Supercritical Fluid Extraction: Principles and Practice*; Butterworth: Stoneham, Mass., USA, 1986.

33. van Leeuwen, P. W. N. M.; Casey, C. P.; Whiteker, G. T., Phosphines as ligands. In *Rhodium Catalyzed Hydroformylation*, van Leeuwen, P. W. N. M.; Claver, C., Eds. Kluwer Academic Publishers: Amsterdam, Netherlands, 2000; pp 63-105.

34. Alvey, L. J.; Meier, R.; Soos, T.; Bernatis, P.; Gladysz, J. A. Syntheses and Carbonyliridium Complexes of Unsymmetrically Substituted Fluorous Trialkylphosphanes: Precision Tuning of Electronic Properties, Including Insulation of the Perfluoroalkyl Groups. *Eur. J. Inorg. Chem.* **2000**, 1975-1983.

CHAPTER V

ORGANIC-AQUEOUS TUNABLE SOLVENTS FOR HOMOGENEOUS CATALYST RECYCLE IN THE HYDROFORMYLATION OF AROMATIC COMPOUNDS

Introduction

In Chapter IV, we examined the hydroformylation of 1-octene in the OATS system. In this chapter, we extend our discussion to another reaction in OATS: the hydroformylation of *p*-methylstyrene. Experiments related both to the reaction and to the product partitioning are currently underway. This chapter presents the results to date and gives a path forward for this ongoing project.

The hydroformylation of *p*-methylstyrene (see Figure 5.1) was chosen to demonstrate the versatility of the OATS system for recycling homogeneous organometallic catalysts. Several important differences exist between this reaction and the hydroformylation of 1-octene presented in Chapter IV. First, we seek to prove the capability of OATS in reactions involving aromatic as well as aliphatic compounds. A significant advantage that comes along with this structural change is the elimination of the isomerization difficulties encountered in Chapter IV.

Another difference between the two reactions is the regiochemistry of the desired product. For aliphatic olefins, such as 1-octene, straight-chain aldehydes are used as chemical feedstocks for fragrance compounds so a high linear to branched ratio (L:B) is desired. Aromatic olefins, such as *p*-methylstyrene, are often used to make

pharmaceuticals or pharmaceutical precursors (e.g. ibuprofen or naproxen). A low L:B is desired for these substrates.

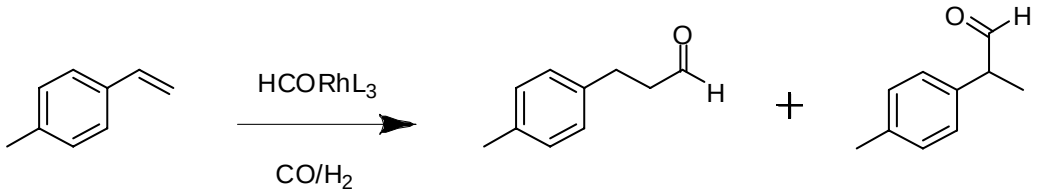

Figure 5.1: The hydroformylation of *p*-methylstyrene.

Experimental

This project employs techniques similar to those presented in Chapter IV. The reaction uses the same catalyst and ligands as the hydroformylation of 1-octene. For the preliminary experiments presented in this work, the reaction vessel and experimental conditions mirrored those used in Chapter IV. Another advantage to the aromatic hydroformylation is the ability to monitor the partitioning with *in situ* high-pressure UV-vis spectroscopy. This technique avoids potential changes in phase behavior due to sampling.

Materials

THF and water used in the experiments were HPLC grade, obtained from Sigma-Aldrich Chemical Company. The HPLC water and THF were degassed using the freeze-pump-thaw method on a Schlenk line apparatus. SFC Grade carbon dioxide (99.99%) was obtained from Air Gas. The CO_2 was further purified to remove trace water using a Matheson (Model 450B) gas purifier and filter cartridge (Type 451). UHP grade syngas (1:1 $CO:H_2$) was obtained from AirGas and used as received. The catalyst (Acetylacetonato)dicarbonylrhodium(I) (98%) as well as the triphenylphosphine

monosulfonate (TPPMS) sodium salt (≥90%) ligand were purchased from Sigma-Aldrich Chemical Company and used as received. The reactant, *p*-methylstyrene (98+%) was purchased from Alfa Aesar and used as received. The branched product, 4-methylphenylacetone (98%), and the linear product, 3-(4-methylphenyl)propionaldehyde (>97%), were purchased from VWR and Rieke Metals, respectively, and used as received.

Apparatus and Procedure

The apparatus and procedure for the reaction experiments was described in Chapter IV. The equipment and techniques used in this chapter are identical to those presented previously, except as noted below.

The initial concentrations of the rhodium catalyst, the ligand, and *p*-methylstyrene were approximately $3x10^{-4}$ mol/L, $3x10^{-3}$ mol/L, and $1.5x10^{-1}$ mol/L, respectively. These concentrations represent a 10:1 molar ratio of ligand to catalyst and a 500:1 molar ratio of substrate to catalyst. These concentrations are more closely aligned with the "standard" hydroformylation conditions recommended by van Leeuwen (T = 70-120ºC, CO and H_2 = 5-25 bar, [Rh] ≈ 1 mmol/L, [alkene] = 0.1-2 mol/L, [P]:[Rh] = 3-100).[1]

The sampling technique for the reaction experiments was slightly different from that presented in the previous chapter. The Parr reactor was equipped with a stainless steel dip tube into the liquid phase. We attached another length of stainless steel tubing to the dip tube valve outside the reactor. We sampled the reactor contents by submerging this tubing into a 10 mL volumetric flask filled with 9 mL of THF, then slowly opening the valve to release the sample into the flask. Volatile reactor contents were recovered by

depressurizing into the THF. This technique, in principle, allows multiple samples without quenching the reaction and could permit kinetic analysis for future experiments.

We analyzed the reactor contents using an Agilent GC-FID (model 6890). External standards of known concentration of *p*-methylstyrene and the linear and branched products were used to calibrate the FID response. We also used GC-MS (Agilent model 5973) to confirm the identity of our products in some of the initial experiments.

The partitioning experiments (not yet complete) will use a high pressure spectroscopy cell as described in Chapters II-III. The response of the UV will be calibrated with samples of known concentrations of either the linear or branched product. The key to these experiments is ensuring that the appropriate phase (water-rich or CO_2-expanded THF-rich) of the resulting biphasic system is visible through the UV cell window. Approximately 3.5 mL of solvent are needed to cover the window, so loadings with different amounts of water and THF will be used along with the phase behavior data of Lazzaroni to measure the product concentration in each phase.[2] Other techniques will be similar to the solvatochromic measurements of Chapter II, except that we shall be concerned with the peak area, rather than λ_{max}.

Results

As this project is ongoing, only limited results are currently available. Some reaction experiments have been performed, and those results are presented here. At the time of this writing, no partitioning experiments have been performed. The reaction data to date are presented in Table 5.1. Concentrations of *p*-methylstyrene and the linear product were determined through GC-FID calibration and sampling. A mass balance was

performed to determine the concentration of the branched product. B:L ratio (rather than L:B) is shown in order to compare larger numbers.

Table 5.1: Reaction results for the hydroformylation of *p*-methylstyrene.

Ligand	T (°C)	Conversion to Aldehydes (%)	Branched to Linear Ratio	TOF (hr^{-1})
TPPMS	120	51 ± 7	0.5 ± 0.6	261 ± 91
	80	67 ± 5	16 ± 4	337 ± 25
	40	56 ± 35	47 ± 43	279 ± 177

These results are based on only two experiments at each temperature, which may explain some of the scatter in the data. Additional replications are needed to determine if the current data, particularly at 40ºC and 120ºC, include outliers.

Path Forward

Because these experiments are ongoing and will likely be completed by my successor, a path forward for future experiments is needed. Additional replications of the experiments presented above, and completion of the partitioning experiments, are obviously a priority. Beyond these experiments, the project should focus on (1) a demonstration of the catalyst recycle, (2) an examination of other solvent mixtures, and (3) an investigation of other ligands.

The key data needed to demonstrate the viability of the OATS system, regardless of the choice of substrate or catalyst, is proof that the catalyst can be recycled and used again without a significant loss of activity. In Chapter IV, we established that the catalyst

could be recycled up to three times without a decrease in activity. A similar study must be performed for this reaction, although the catalyst and ligand are the same. After completing the studies related to the solvent and ligand (see below), the best system should be evaluated for a minimum of five recycles.

The work presented in Chapter IV focused on a mixed solvent of THF and water for the reaction. This system was chosen due to favorable separation upon CO_2 addition. Indeed, the catalyst recovery and recycle are the key features of the OATS system, so the separation is important. The OATS system represents a holistic approach to reactions and separations, and as such, we must consider factors influencing both the reaction and the separation. A key variable that is yet to be examined thoroughly in the OATS system is the choice of organic solvent. As we demonstrated in Chapters II-III, small changes in solvent properties can impact reaction rates significantly. The logical solvent choices yet to be explored are acetonitrile+water and dioxane+water, due to established phase behavior upon CO_2 addition.[2] If the rate or selectivity of the reaction is altered positively by a change in solvent, the process economics could be improved despite a slightly poorer separation.

Finally, a further examination of the choice of ligand may be important. Triphenylphosphine and its derivatives have been used thus far on this project, and are quite common in industrial hydroformylations. For the work completed so far in this chapter, TPPMS was chosen because it represents a compromise between the high activity and selectivity of TPP and the favorable partitioning of TPPTS (see Chapter IV for structures). Another potential ligand for future work is a water-soluble analog of

TunaPhos. This ligand shows high regioselectivity and can also be used for future asymmetric reactions (see Chapter VI for recommended asymmetric reactions).[3, 4]

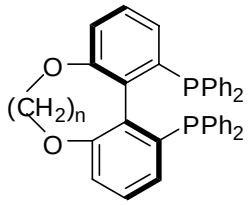

Figure 5.2: TunaPhos ligand structure.

References

1. van Leeuwen, P. W. N. M.; Casey, C. P.; Whiteker, G. T., Phosphines as ligands. In *Rhodium Catalyzed Hydroformylation*, van Leeuwen, P. W. N. M.; Claver, C., Eds. Kluwer Academic Publishers: Amsterdam, Netherlands, 2000; pp 63-105.

2. Lazzaroni, M. J.; Bush, D.; Jones, R.; Hallett, J. P.; Liotta, C. L.; Eckert, C. A., High-pressure phase equilibria of some carbon dioxide-organic-water systems. *Fluid Phase Equilibria* **2004,** *224*, 143.

3. Tang, W.; Wu, S.; Zhang, X., Enantioselective hydrogenation of tetrasubstituted olefins of cyclic *β*-(Acylamino)acrylates. *J. Am. Chem. Soc.* **2003,** *125*, 9570.

4. Wu, S.; Wang, W.; Tang, W.; Lin, M.; Zhang, X., Highly enantioselective hydrogenation of enol acetates catalyzed by Ru-TunaPhos complexes. *Org. Lett.* **2002,** *4* (25), 4495.

CHAPTER VI

CONCLUSIONS AND RECOMMENDATIONS

Gas-expanded liquids offer many of the advantages of both organic liquids and supercritical fluids. In this thesis, we have shown the results of several studies related to the properties of GXLs as solvents as well as their potential industrial applications via the OATS process. This chapter focuses on the major findings of the thesis and suggests directions for future research.

Kinetic and solvatochromic probes of GXLs

In Chapters II-III, we used an innovative approach to combine kinetic and solvatochromic studies of GXL local properties. Through this approach, we gained both qualitative and quantitative insight into the molecular behavior of these solvents. In Chapter II, we used a multiparameter model to explain the solvent effects on a Diels-Alder reaction in GXLs in terms of polarity and hydrogen bonding between the solutes and the solvent. In doing this, we identified several specific interactions that may affect the kinetics of the reaction. In Chapter III, we used kinetic and solvatochromic probes of local solvent polarity to measure the effects of local composition enhancement on the reaction.

The findings presented in these chapters can stimulate future work with GXLs. Knowing that these specific interactions can occur allows future researchers either to exploit these interactions for particular processes (e.g. in the case of Lewis acid catalysis by CO_2) or to avoid potentially harmful or expensive mistakes. Furthermore, the techniques developed in this work are widely applicable for a range of solvents.

Application of these techniques to other neoteric solvents and particularly solvent mixtures, such as deep eutectic solvents, is straightforward.

Diels-Alder reaction

One area of particular interest related to the continuation of this work is broadening the study to include a wider range of gas-expanded solvents. A major limitation in this effort has been the choice of reactions, especially the Diels-Alder reaction of anthracene and PTAD. While the high reactivity of PTAD is an advantage in terms of decreasing reaction times for the experiments, it becomes a disadvantage in terms of comparing rates in other solvents. As reported in Chapter II, PTAD reacts with many solvents commonly used in GXL studies.

We did examine the reaction of anthracene and PTAD in ethane-expanded acetonitrile (see Figure 6.1). Since ethane is not as soluble in acetonitrile as is CO_2, much higher pressures are needed to achieve high ethane mole fractions in the liquid phase.[1] The choice of expansion gas does appear to have some effect, at least at low mole fractions of gas, but further experiments at higher ethane loadings are needed to determine the importance of this effect.

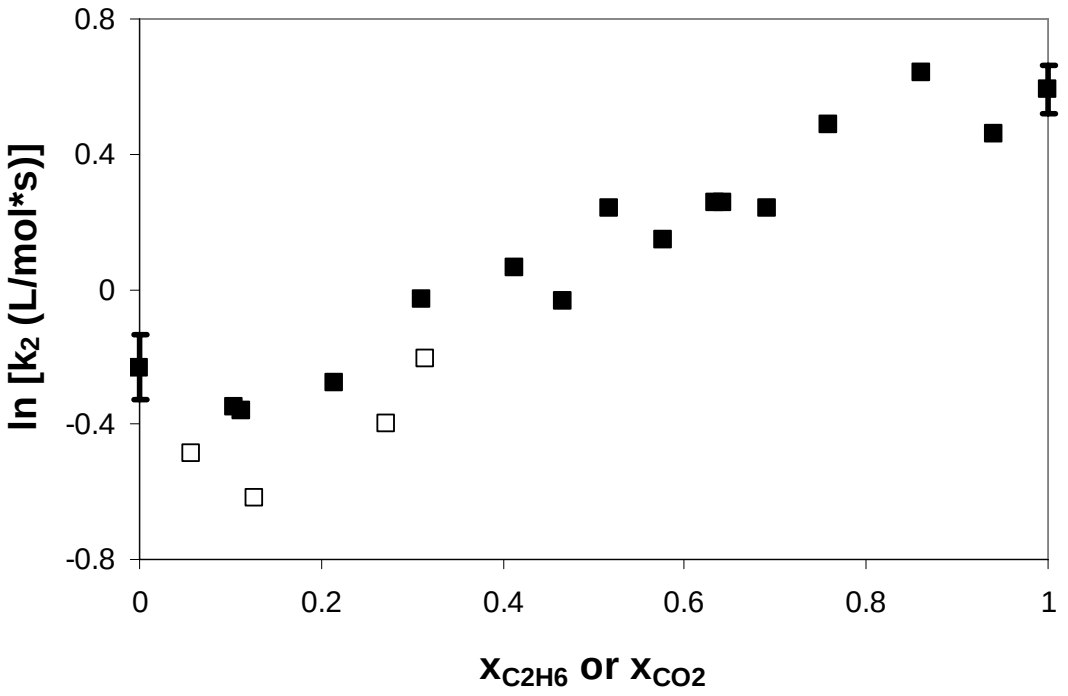

Figure 6.1: Effect of expansion gas on Diels-Alder rate. Acetonitrile expanded with CO_2 (■) or ethane (□).

An important area for future work is to use a different reaction that is more versatile in terms of solvent selection. Similar reactions that should meet this goal are presented in Figure 6.1.[2-8] The reactions presented in this figure can be analyzed by either UV-Vis spectroscopy or fluorescence spectroscopy. A key step in any such study is to determine the stability of the reactants in the solvents of interest prior to attempting kinetic measurements.

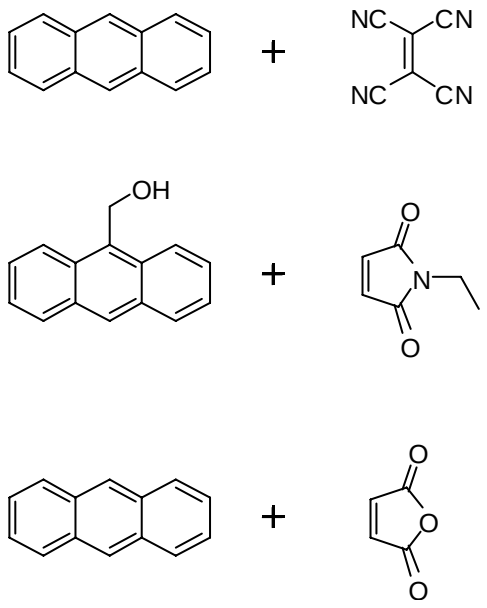

Figure 6.2: Alternate Diels-Alder reactions.

Another interesting course for this work would be a more comprehensive examination of our hypothesized specific interactions involving the solutes and the solvent. Molecular dynamics simulations may be able to provide additional evidence to support the formation of the extended-dipole complex or Lewis acid effects. Indeed, work is underway in the Eckert-Liotta group to probe these interactions computationally. From an experimental standpoint, low temperature ^{13}C NMR may be an option to examine these complexes.[9]

<u>S_N2 reaction</u>

In contrast to the Diels-Alder reaction, the S_N2 reaction should be amenable to a range of gas-expanded polar aprotic solvents. The only apparent limitations to this reaction with such solvents are the use of UV-Vis spectroscopy and the ability of the gas-expanded solvent to support the polar solutes involved in this reaction. Provided the solvent does not have a UV signature in the range of 200-400 nm, analysis of the reaction

should not be an issue. Beginning with a pure (pre-expansion) solvent of polarity similar to or higher than acetonitrile should allow data collection over a wide range of solvent composition. The Kamlet-Taft solvatochromic properties of other solvents that may prove interesting are shown in Table 6.1, with acetonitrile as a reference point.[10] Although these solvents have similar properties, specific interactions may differ, generating potentially useful information.

Table 6.1: Potential S_N2 solvents and their Kamlet-Taft parameters.

Solvent	π^*	α	β
Acetonitrile	0.75	0.19	0.4
Tetrahydrofuran	0.58	0	0.55
Dioxane	0.55	0	0.37
Chloroform	0.58	0.2	0.1

Hydroformylation in OATS

Our work so far in the OATS system has shown tremendous potential. In Chapter IV, we demonstrated an improvement in the turnover frequency of the catalyst in the mixed solvent of nearly two orders of magnitude over the comparable biphasic reaction. We have also shown that we can recycle the catalyst three times without a significant decrease in activity. Our preliminary results for the hydroformylation of *p*-methylstyrene (Chapter V) are promising as well.

Although enzyme catalysis in OATS continues to be an area of great interest in the Eckert-Liotta and Bommarius groups, I shall focus my recommendations on

organometallic catalysis due to my limited experience with the biocatalysis aspects of this project.

The hydroformylation of *p*-methylstyrene presents a good opportunity to demonstrate the versatility of the OATS system. Experiments related to this reaction are underway, and a recommended path forward for those experiments is given in Chapter V. The solvent studies are particularly recommended due to the lack of reaction studies in the other (non-THF) "OATS solvents": acetonitrile and dioxane. Although the phase behavior may not be quite as favorable, the solvent effects on the reaction are yet to be determined.[11]

Beyond the recommendations in Chapter V, reactions involving chiral species should be the next major area of study. An important asymmetric hydroformylation is the hydroformylation of (5-methoxy-1-naphthyl)ethylene, a precursor for the pharmaceutical *S*-naproxen (see Figure 6.3).[12] Other target reactions for the OATS system include hydrogenations (including asymmetric transfer hydrogenations) and epoxidations.

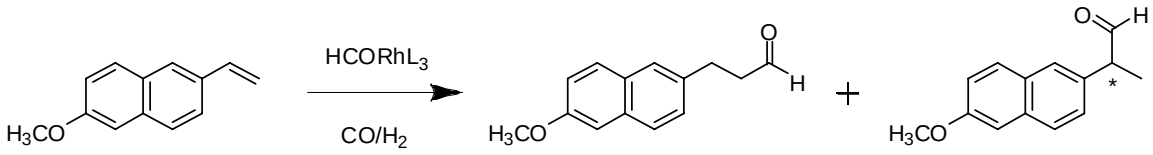

Figure 6.3: Hydroformylation of (5-methoxy-1-naphthyl)ethylene. S-naproxen (branched chiral isomer at far right) is the desired product.

A study examining the effectiveness of OATS with chiral, water-soluble ligands, such as sulfonated BINAP, SYNPHOS, (sulfonylamino)methylpyrrolidine derivatives, and bis(sulfonamide)-cyclohexane-1,2-diamine may be useful as well.[13-16]

References

1. Kordikowski, A.; Schenk, A. P.; Van Nielen, R. M.; Peters, C. J., Volume expansions and vapor-liquid equilibria of binary mixtures of a variety of polar solvents and certain near-critical solvents. *J. Supercritical Fluids* **1995,** *8*, 205.

2. Konovalov, A. I.; Breus, I. P.; Sharagin, I. A.; Kiselev, V. D., Study of solvation effects in Diels-Alder reactions of 4-phenyl-1,2,4-triazoline-3,5-dione with anthracene and trans,trans-1,4-diphenyl-1,3-butadiene. *Zhurnal organicheskoi khimii* **1979,** *15* (2), 361.

3. Garcıa, J. I.; Mayoral, J. A.; Salvatella, L., Solvent effects on the 9-hydroxymethylanthracene + *N*-ethylmaleimide Diels-Alder reaction. A theoretical study. *J. Org. Chem.* **2005,** *70*, 1456.

4. Wang, B.; Han, B.; Jiang, T.; Zhang, Z.; Xie, Y.; Li, W.; Wu, W., Enhancing the rate of the Diels-Alder reaction using CO_2 + ethanol and CO_2 + *n*-hexane mixed solvents of different phase regions. *J. Phys. Chem. B* **2005,** *109*, 24203.

5. Qian, J.; Timko, M. T.; Allen, A. J.; Russell, C. J.; Winnik, B.; Buckley, B.; Steinfeld, J. I.; Tester, J. W., Solvophobic acceleration of Diels-Alder reactions in supercritical carbon dioxide. *J. Am. Chem. Soc.* **2004,** *126*, 5465.

6. Bose, A. K.; Manhas, M. S.; Ghosh, M. S., Mamta; Raju, V. S.; Bari, S. S.; Newaz, S. N.; Banik, B. K.; Chaudhary, A. G.; Barakat, K. J., Microwave-induced organic reaction enhancement chemistry. 2. Simplified techniques. *J. Org. Chem.* **1991,** *56* (25), 6968.

7. Kiselev, V. D.; Kashaeva, E. A.; Potapova, L. N.; Iskhakova, G. G., Diels-Alder reaction between naphthalene and *N*-phenylmaleimide

under mild conditions. *Russ. Chem. Bull., Int. Ed.* **2004,** *53* (1), 51.

8. Atherton, J. C. C.; Jones, S., Diels-Alder reactions of anthracene, 9-substituted anthracenes and 9,10-disubstituted anthracenes. *Tetrahedron* **2003,** *59*, 9039.

9. Denisov, G. S.; Gindin, V. A.; Golubev, N. S.; Ligay, S. S.; Shchepkin, D. N.; Smirnov, S. N., NMR study of proton location in strongly hydrogen bonded complexes of pyridine as influenced by solvent polarity. *J. Mol. Liq.* **1995,** *67*, 217.

10. Marcus, Y., The properties of organic liquids that are relevant to their use as solvating solvents. *Chem. Soc. Rev.* **1993**, 409.

11. Lazzaroni, M. J.; Bush, D.; Jones, R.; Hallett, J. P.; Liotta, C. L.; Eckert, C. A., High-pressure phase equilibria of some carbon dioxide-organic-water systems. *Fluid Phase Equilibria* **2004,** *224*, 143.

12. Rajurkar, K. B.; Tonde, S. S.; Didgikar, M. R.; Joshi, S. S.; Chaudhari, R. V., Environmentally benign catalytic hydroformylation-oxidation route for naproxen synthesis. *Ind. Eng. Chem. Res.* **2007**, In press.

13. Touati, R.; Ratovelomanana-Vidal, V.; Hassinea, B. B.; Genet, J.-P., Synthesis of enantiopure (R)-(-)-massoialactone through ruthenium-SYNPHOS asymmetric hydrogenation. *Tetrahedron: Asymmetry* **2006,** *17*, 3400.

14. Cortez, N. A.; Aguirre, G.; Parra-Hake, M.; Somanathan, R., Water-soluble chiral monosulfonamide-cyclohexane-1,2-diamine-RhCp* complex and its application in the asymmetric transfer hydrogenation (ATH) of ketones. *Tetrahedron Letters* **2007,** *48*, 4335.

15. Canivet, J.; Suss-Fink, G., Water-soluble arene ruthenium catalysts containing sulfonated diamine ligands for asymmetric transfer hydrogenation of a-aryl ketones and imines in aqueous solution. *Green Chem.* **2007,** *9*, 931.

16. Wan, K.-t.; Davis, M. E., Ruthenium(II)-sulfonated BINAP: a novel water-soluble asymmetric hydrogenation catalyst. *Tetrahedron: Asymmetry* **1993,** *4* (12), 2461.

APPENDIX A

ELECTRONIC EFFECTS FOR OATS LIGANDS

Introduction

In Chapter 4, we discussed the hydroformylation of 1-octene in the OATS system using three phosphine ligands: triphenylphosphine (TPP), triphenylphosphine monosulfonate (TPPMS), and triphenylphosphine trisulfonate (TPPTS). We reported differences in the ratios of aldehydes (desired products) to isomers (undesired products) for each ligand. We hypothesized that these differences were related to electronic effects from the additional sulfonate groups added to the ligand. We made additional efforts to prove or disprove this hypothesis with the ligands in this work, and the results of these efforts are presented in this appendix.

Ligand structure can significantly impact conversion and selectivity in rhodium-catalyzed hydroformylations.[1-3] Electron-withdrawing phosphines have been shown to increase isomerization rates.[4]

In the olefin hydroformylation reaction mechanism proposed by Bianchini, the phosphine ligand must dissociate for the reaction to occur.[5] By decreasing the electronic density on the phosphine, the rhodium is less electron rich, decreasing its back donation ability with CO. This makes isomerization a more competitive pathway as it is easier for the alkene complexation to take place. Then CO insertion (to form the aldehyde) directly competes with beta-elimination (to form alkene isomers).[6]

A number of methods have been used in the literature to measure experimentally or to estimate the pK_a of phosphines, including titration, ^{31}P NMR, calorimetry, and

computational methods.[7-15] The pK_a of the phosphine can then be correlated to the electronic density of the phosphine, providing a means of comparing the ligands. We used ^{31}P NMR and Spartan calculations to determine the relative basicities of the phosphine ligands.

Experimental

For the ^{31}P NMR measurements, we weighed approximately 10 mg of each ligand into separate NMR tubes. We then added approximately 1 mL 70% THF, 30% D_2O (which mimics our reaction solvent) to each tube. After flushing the headspace with argon, we sealed the tube and measured the ^{31}P NMR.

We used the Spartan software package (Version 04). 1,0,0 and the lowest energy (i.e. most stable) conformers and their relative energy were identified using Hartree-Fock (HP – 3.21G*) data sets to calculate the Mulliken charge on the phosphorus for each ligand. Triphenylphosphine disulfonate (TPPDS) was substituted for TPPTS due to the inability of the program to handle extensive charges.

Results

Results for the ^{31}P NMR experiments are shown in Figure A.1. The chemical shift of the phosphine changes from -4.88 (TPP) to -4.49 (TPPMS) to -4.1 (TPP). There is a clear trend between δ and the isomerization. The upfield shift with increasing sulfonation suggests decreasing electron density (lower basicity) of the phosphine. This observation is in agreement with the literature reports supporting increased isomerization with more electron-withdrawing phosphines.[4] Note that the measurements were not conducted at a constant ionic strength or pH, so the shift may be due in part to these effects.[7]

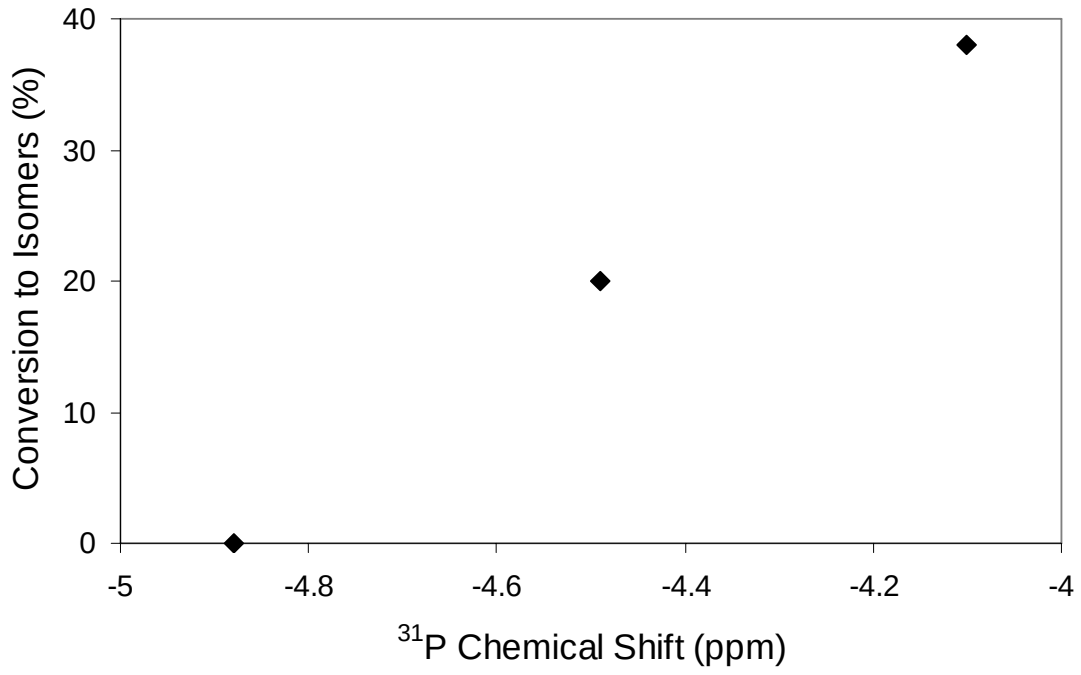

Figure A.1: Isomerization versus ^{31}P chemical shift for TPP, TPPMS, and TPPTS.

The results of our Spartan calculations are given in Table A.1. The Mulliken charge density on the P of the ligands increases slightly with increasing sulfonation. The significance of the difference between the values is questionable. Also, Spartan is not the best program to handle charged molecules and this may be a limitation. The calculations were performed with sulfonic acid (in place of negative sulfonate group). The phosphorus electron density did not show much difference with the one calculated for the sulfonate analogs. We observed small changes in the geometry of the ligands, as measured by the C-P-C angles. HOMO and LUMO density maps (not shown) also show differences.

Table A.1: Spartan calculation results for TPP, TPPMS, and TPPDS.

Ligand	Mulliken charge of P	C-P-C dihedral angle 1	C-P-C dihedral angle 2	C-P-C dihedral angle 3
TPP	1.032	102.36	102.36	102.36
TPPMS	1.034	102.44	101.43	103.07
TPPDS	1.040	104.35	102.46	99.91

Conclusions

The NMR study supports that the phosphorus electron density decreases with increasing sulfonation. As widely reported in the literature, such decrease in electron density will result in increased isomerization. Unfortunately, the calculations using Spartan (HF-3.21G*) data sets could not confirm our experimental results. This discrepancy can be attributed to the limitation of the program when it comes to handling molecules that are not neutral.

References

1. Suomalainen, P.; Laitinen, R.; Jääskeläinen, S.; Haukkaa, M.; Pursiainen, J. T.; Pakkanen, T. A., Multidentate phosphanes as ligands in rhodium catalyzed hydroformylation of 1-hexene *J. Mol. Cat. A: Chem.* **2002,** *179*, 93.

2. Suomalainen, P.; Reinius, H. K.; Riihimäki, H.; Laitinen, R. H.; Jääskeläinen, S.; Haukkaa, M.; Pursiainen, J. T.; Pakkanen, T. A.; Krause, A. O. I., Hydroformylation of 1-hexene and propene with in situ formed rhodium phosphine catalysts. *J. Mol. Cat. A: Chem.* **2001,** *169* 67.

3. Wang, X.; Fu, H. Y.; Li, X.; Chen, H., Hydroformylation of high olefin in biphasic catalytic system: effect of electronic and steric factor of phosphine ligands. *Catal. Comm. 5* **2004**, 739.

4. van Leeuwen, P. W. N. M.; Casey, C. P.; Whiteker, G. T., Phosphines as ligands. In *Rhodium Catalyzed Hydroformylation*, van Leeuwen, P. W. N. M.; Claver, C., Eds. Kluwer Academic Publishers: Amsterdam, Netherlands, 2000; pp 63-105.

5. Bianchini, C.; Lee, H. M.; Meli, A.; Vizza, F., In situ high-pressure $^{31}P\{^{1}H\}$ NMR studies of the hydroformylation of 1-hexene by $RhH(CO)(PPh_3)_3$. *Organometallics* **2000,** *19*, 849.

6. Pollet, P. Personal communication, 2007.

7. Pestovsky, O.; Shuff, A.; Bakac, A., Protonation constants for triarylphosphines in aqueous acetonitrile solutions. *Organometallics* **2006,** *25*, 2894.

8. Bortoluzzi, M.; Annibale, G.; Marangoni, G.; Paolucci, G.; Pitteri, B., ^{31}P NMR and DFT studies on square-planar bis(diphenylphosphinoethyl)phenylphosphine (triphos) complexes of Pt(II) with pyridines and anilines. *Polyhedron* **2006,** *25*, 1979.

9. Bush, R. C.; Angelici, R. J., Phosphine basicities as determined by enthalpies of protonation. *Inorg. Chem.* **1988,** *27* (4), 681.

10. Henderson, W. A. J.; Streuli, C. A., The basicity of phosphines. *J. Am. Chem. Soc.* **1960,** *82*, 5791.

11. Kovacevic, B.; Maksic, Z. B., High basicity of phosphorus-proton affinity of tris-(tetramethylguanidinyl)phosphine and tris-(hexamethyltriaminophosphazenyl)phosphine by DFT calculations. *Chem. Commun.* **2006**, 1524.

12. Li, J.-N.; Liu, L.; Fu, Y.; Guo, Q.-X., What are the pK_a values of organophosphorus compounds? *Tetrahedron* **2006,** *62*, 4453.

13. Streitwieser, A.; McKeown, A. E.; Hasanayn, F.; Davis, N. R., Basicity of some phosphines in THF. *Org. Lett.* **2005,** *7* (7), 1259.

14. Streuli, C. A., Determination of basicity of substituted phosphines by nonaqueous titrimetry. *Anal. Chem.* **1960,** *32* (8), 985.

15. Suresh, C. H.; Koga, N., Quantifying the electronic effect of substituted phosphine ligands via molecular electrostatic potential. *Inorg. Chem.* **2002,** *41*, 1573.

VITA

Jackson Walker Ford born in Amory, Mississippi on June 13, 1979 to Terry and Lee Ellen Ford. He was raised in Columbus, Mississippi, and attended Columbus High School. He received his B.S. in chemical engineering from Mississippi State University in 2001, and his M.S. in chemical engineering, also from Mississippi State University, in 2004. Since then, he has worked under the direction of Dr. Charles Eckert and Dr. Charles Liotta in pursuit of a Ph.D. in chemical engineering at the Georgia Institute of Technology. He enjoys spending time with his wife Christine, as well as their extended families, and playing tennis and golf. A list of selected publications follows:

Jackson W. Ford, Jie Lu, Charles L. Liotta, Charles A. Eckert. "Solvent effects on the kinetics of a Diels-Alder reaction in gas-expanded liquids." Accepted for publication in *Industrial & Engineering Chemistry Research*.

Jason P. Hallett, Jackson W. Ford, Rebecca S. Jones, Pamela Pollet, Colin A. Thomas, Charles L. Liotta, Charles A. Eckert. "Hydroformylation catalyst recycle with gas-expanded liquids." Submitted to *Industrial & Engineering Chemistry Research*.

Jackson W. Ford, Malina E. Janakat, Jie Lu, Charles L. Liotta, Charles A. Eckert. "Local polarity in CO_2-expanded acetonitrile: substitution reaction and solvatochromic probes." Submitted to the *Journal of Organic Chemistry*.

Jack Ford, W. Todd French, Rafael Hernandez, Emily Easterling, Mark Zappi, Christine Morrison, Margarita Licha, and Lewis R. Brown. "A system for cultivating anaerobic carbon monoxide utilizing bacteria." *Bioresource Technology* **2008**, *99*, 638-643.

Jack Ford, Rafael Hernandez, and Mark Zappi. "Bench-scale evaluation of advanced oxidation processes for treatment of a cyanide-contaminated wastewater from an engine manufacturing facility." *Environmental Progress* **2006**, *25*, 32-38.